Aircraft System Noise of the NASA D8 Subsonic Transport Concept

Ian A. Clark* and Russell H. Thomas†
NASA Langley Research Center, Hampton, VA 23681 USA

Yueping Guo‡
NEAT Consulting, Seal Beach, CA 90740 USA

A vehicle-level noise assessment has been performed for the NASA D8 concept aircraft (ND8) in the NASA Advanced Air Transport Technology Project portfolio. The NASA research-level Aircraft NOise Prediction Program (ANOPP-Research) was used to predict the noise from each source component on the ND8 to build up a noise estimate for the full aircraft. The propulsion airframe aeroacoustic (PAA) effects of the ND8, namely boundary layer ingestion (BLI) with its influence on fan noise, and the noise shielding, reflection, and diffraction mechanisms of the unconventional airframe, were empirically modeled using experimental data. Far Term noise reduction technology concepts were modeled and added to the noise prediction to evaluate the low-noise potential of the ND8 in the Far Term timeframe. Results indicate that the increase in fan noise due to boundary layer ingestion, as well as the lack of aft shielding, prevent the aircraft from approaching NASA's noise goals for either the Mid or Far Term. The aircraft achieves margins to Stage 4 of only 9.4 and 17.3 EPNdB in the Mid and Far Term configurations, respectively, compared with goals of 32-42 EPNdB in the Mid Term and 42-52 EPNdB in the Far Term.

I. Introduction

The NASA Advanced Air Transport Technology (AATT) Project is aimed at the development and demonstration of advanced technologies for aircraft systems that could meet aggressive goals for fuel burn, noise, and emissions. In the Mid Term time frame (2025-2035), the fuel burn reduction goal is 50-60% relative to a best-in-class 2005 aircraft, and the noise goal is 32-42 EPNL dB (Effective Perceived Noise Level) cumulative below the Stage 4 FAA noise requirement; the emission goal is a reduction of 80% in NOx (oxides of nitrogen) levels below the CAEP 6 (Committee on Aviation Environmental Protection) standard [1]. In addition to more stringent fuel burn and NOx reductions, the Far

A compilation of work presented as Paper 2018-3124 at the 2018 AIAA/CEAS Aeroacoustics Conference, Atlanta, GA, 25-29 June 2018, and as Paper 2019-2427 at the 2019 AIAA/CEAS Aeroacoustics Conference, Delft, The Netherlands, 20-23 May 2019

*Research Aerospace Engineer, Aeroacoustics Branch, MS 461, AIAA Member, ian.a.clark@nasa.gov.
†Senior Research Engineer, Aeroacoustics Branch, MS 461, AIAA Associate Fellow.
‡NEAT Consulting, 3830 Daisy Circle, AIAA Associate Fellow.

Term (2035 and beyond) goal for noise reduction is 42-52 EPNL dB cumulative below Stage 4. The AATT Project seeks to mature technology that will support development of new aircraft products that meet or exceed Mid Term and Far Term metrics. The NASA D8 (ND8, Figure 1) was developed primarily as a technology collector for AATT to serve as a platform to assess the incremental benefits of including certain technologies on an airframe. The ND8 concept is based on the Massachusetts Institute of Technology (MIT)/Aurora Flight Sciences D8 aircraft first developed under a 2008 NASA Research Announcement [2] and later updated by Drela [3]. Yutko et al. [4] undertook a comprehensive conceptual design of the MIT/Aurora D8. The designation NASA D8 (ND8) is intended to differentiate the NASA model of the D8 from the MIT/Aurora D8 model, since different tools and assumptions were used to develop the models. The ND8 concept is not fully designed to serve in the National Airspace System, but rather is designed to resemble the overall D8 concept with details provided by NASA tools and models for aircraft design, analysis, and optimization. More details of the ND8 design are given in Section III.

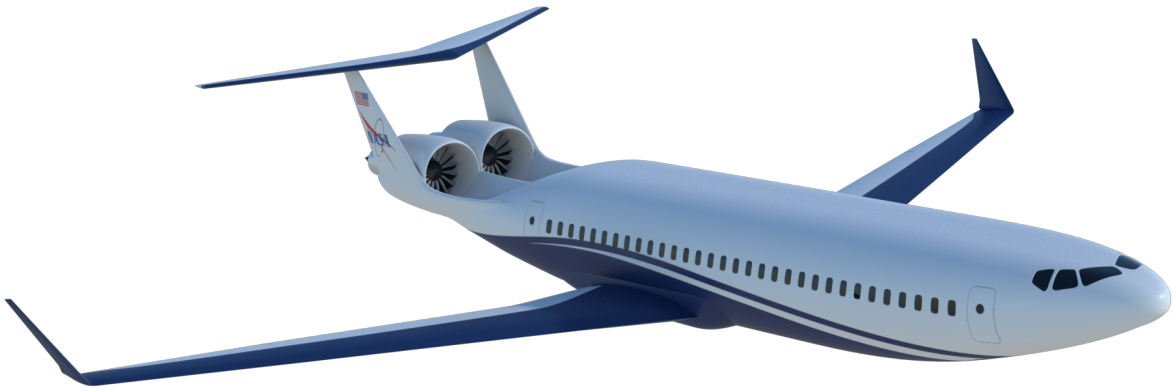

Fig. 1 Artist rendering of the NASA D8 subsonic transport concept.

The combined fuel consumption, emissions, and noise goals of AATT will likely require a change in aircraft configuration from the traditional "tube and wing" design that has persisted throughout many years of advancements in technology, structures, materials, and aerodynamic design [5]. The cylindrical fuselage provides an effective pressure vessel to resist pressure loading of the cabin while flying at high altitudes. A noncylindrical fuselage experiences additional stresses and bending moments while under pressure, which necessitates structural reinforcements that can be heavy and expensive. The ND8 features a twin-aisle lifting body fuselage [4]. This "double-bubble" design retains a similar load path through the fuselage structure by using two partial cylinders braced with faired tension rods in the cabin [6]. This design enables a wide fuselage, which leads to increased passenger capacity, faster boarding times, and additional lift generation. The lift generated by the fuselage has several impacts on the design of the airframe, namely the reduction of wing area in proportion to the size of the fuselage, and a decrease of horizontal tail area due to the increased lift acting near the front of the aircraft, which contributes a positive pitching moment [4].

The ND8 concept calls for placement of the engines at the aft dorsal location on the fuselage to take advantage of fuel savings arising from boundary layer ingestion (BLI). The ND8 engines ingest the boundary layer moving over the top of the fuselage - about 40% of the total boundary layer surrounding the fuselage [7]. BLI leads to increased propulsive efficiency by reducing the flow velocity differential between the propulsive airstream and the free stream flow, compared to a traditional engine under the wing configuration [7]. Much work has been done on the aerodynamic impact of such a design [7–11] and in designing an "inflow-distortion-tolerant" fan, but the acoustic impact of this configuration has not been wholly addressed. De la Rosa Blanco and Hileman [12] published a system level noise assessment of the Aurora Flight Sciences/MIT D8 design using correlations that were self-programmed based on documentation of the NASA Aircraft NOise Prediction Program (ANOPP). The use of self-programmed noise models that were intended for conventional tube-and-wing aircraft yields high uncertainty for this noise prediction of an unconventional configuration. The effect of incorporating boundary layer ingestion was limited to increased shielding with the engines placed at the aft dorsal location. A full conceptual design of the Aurora/MIT D8 also featured a noise assessment [4]. Boundary layer ingestion was incorporated into the design, and noise was predicted with and without this feature. The configuration change to shift the engines from the underwing location (no BLI) to the aft dorsal location (to enable BLI) is reported to provide a noise reduction of approximately 7 EPNdB cumulative on a system level. It is assumed by the authors of this study that Yutko et al. [4] computed the acoustic BLI effect considering only the system benefits associated with reduced engine requirements, reduced weight, and favorable placement of the engines above the fuselage to take advantage of noise shielding. Prior experiments have shown that boundary layer ingestion, and inflow distortion in general, leads to significantly increased fan noise due to unsteady loading of the fan blades [13–15]. Therefore, a complete, credible noise prediction must include all positive and negative propulsion airframe aeroacoustic (PAA) effects: boundary layer ingestion, shielding, reflection, and diffraction.

In support of the NASA goal to quantify the expected noise benefit from unconventional configurations in the AATT portfolio, this work presents a system level noise assessment of the proposed ND8, which may give insight into the noise characteristics of a D8 vision system. It is the goal of this study to quantify and account for all aspects of the ND8 design that potentially impact its acoustic performance, including the aforementioned PAA effects. All relevant features of the design will be incorporated into the prediction, including noise from the high lift system, landing gear, wings, tail, engine fan, engine core, and jet, along with the PAA effects on engine noise sources. In addition, a Far Term technology roadmap will be presented in order to evaluate NASA's portfolio of noise reduction technology concepts on this aircraft configuration, and to determine the aircraft's ability to meet Far Term noise goals.

II. Noise Prediction Methodology

The NASA ANOPP [16] and ANOPP2 [17] codes provide the framework for the current noise prediction study. The models and methods contained in ANOPP are under continuous development, and the research-version code

(ANOPP-Research) used in this study contains several models not present in the released version of ANOPP. The methodology adopted over the last several years during the Environmentally Responsible Aviation (ERA) Project places heavy emphasis on the use of relevant experimental data and physics-based methods, which are compatible with complex, unconventional aircraft. This is reflected in the addition of the GUO-LG [18], GUO-FLAP, and GUO-LE [19] modules into ANOPP-Research. The current publicly available version of ANOPP features mainly empirical or semiempirical relations, which are more suited to conventional aircraft design philosophies. The progression and development of the noise prediction process during the ERA Project is discussed in detail in Thomas et al. [20]. An additional key advancement in recent years has been the ability to directly predict PAA effects, including engine noise shielding and reflection effects of the airframe, using experimental databases and unique data processing tools. June et al. [21] discuss the uncertainty in the system noise prediction of a hybrid wing-body aircraft concept using the same or similar methods to those used in the present study.

Figure 2 shows the overall noise prediction process and methods. ANOPP-Research L31v6 is used within the ANOPP2 framework. A noise prediction begins with detailed information about the aircraft geometry, engine design and performance, and flight path. Several experimental datasets contribute to the design of the aircraft, as well as the noise source definitions. Integrated Technology Demonstration (ITD) efforts, summarized by Nickol and Haller [22], were undertaken during the last three years of the ERA Project, and those results are also used to inform the models for advanced technologies associated with vehicles in the AATT portfolio. Each noise source is predicted individually and follows the flight path for each certification point, which is determined by the unique aircraft design. PAA effects are evaluated for each engine source using experimental data before the noise is propagated through the atmosphere to ground observers. ANOPP provides one-third octave band spectra for each source and observer time as the aircraft flies overhead.

The final result of a noise prediction is the cumulative noise metric, which is described in Figure 3. The noise metrics reported for all predictions are calculated as defined in 14 CFR Part 36 [23]. In order to obtain Federal Aviation Administration (FAA) certification to fly, the noise of an aircraft may not exceed certain noise levels defined using the Effective Perceived Noise Level (EPNL), computed by integrating tone-corrected perceived noise level (PNLT) over time. Noise metrics must be met for the approach, lateral, and flyover locations, which correspond to the stages of flight with the greatest noise impact on communities surrounding airports. The maximum allowable EPNL at each certification point is defined by the aircraft weight and number of engines. These same metrics are used to evaluate future aircraft and noise reduction concepts in order to quantify their value on a system level using accepted standards. Noise predictions are performed at each certification point, resulting in individual EPNLs, which are then combined to arrive at the cumulative EPNL. The latest standard for certification is termed Stage 5. However, the NASA noise goals referenced in this and previous publications are written in reference to Stage 4 certification levels. For the advanced aircraft and noise reduction technologies evaluated in this study, the certification levels are reported as margins below

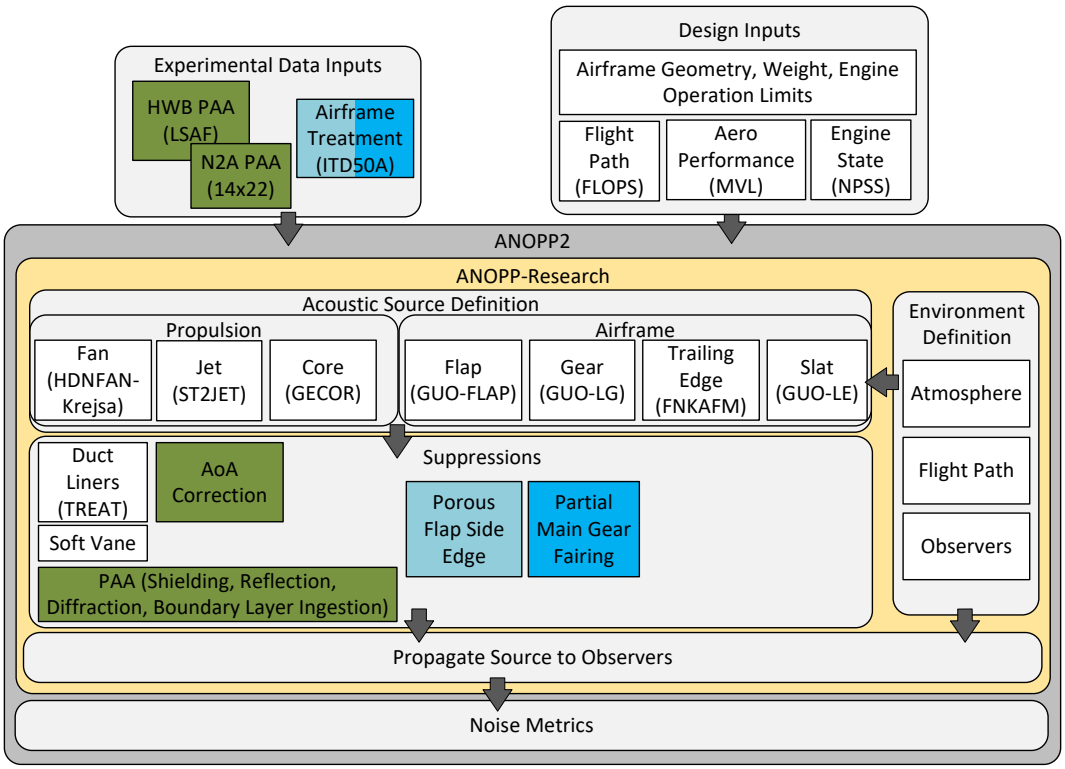

Fig. 2 Overview of the prediction process used in the current study.

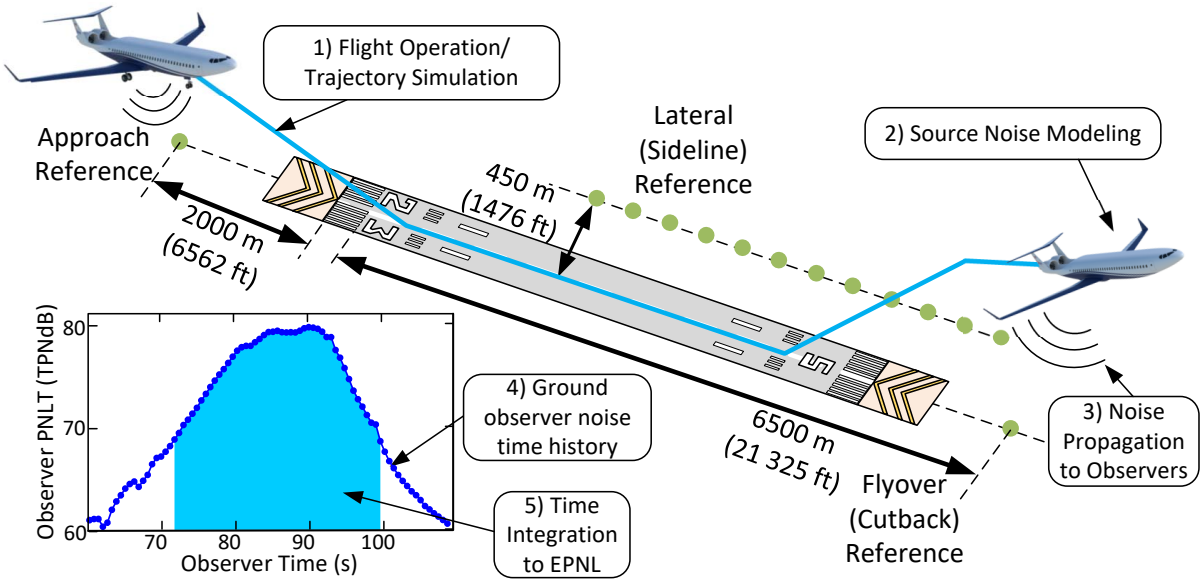

Fig. 3 Noise certification points with prediction methodology.

Stage 4 to clearly define the benefit of these concepts in terms of NASA goals and in relation to previous studies.

III. ND8 Design

The ND8 was designed to carry 180 passengers a distance of 3000 nautical miles, with a cruise Mach number and altitude of 0.785 and 37,000 feet, respectively. The design balanced field length was 8000 feet. This mission is similar to that of the Boeing 737-800, which serves as the reference vehicle to the ND8. The aircraft design and sizing were performed by Marien et al. [7], and overall weight and size parameters are given in Table 1. As mentioned previously, the ND8 was not designed as a vision system to serve in the National Airspace System, but rather to complete the given mission while retaining the overall configuration and features of the MIT/Aurora D8. The design optimization was set up to minimize block fuel for the design mission. As such, the ND8 was not optimized for noise reduction, for example, by tailoring the engine design and operating conditions to minimize noise. Advanced aerodynamics, materials, and propulsion system assumptions were made consistent with a 2035 entry-into-service date. Tools for the vehicle design included the NASA Flight Optimization System (FLOPS) [24] and Numerical Propulsion System Simulation (NPSS) [25]. A rendering showing the design elements of the ND8 is shown in Figure 4.

Table 1 ND8 overall weight and size parameters.

Takeoff Gross Weight	141610 lb
Wing chord (max)	14.7 ft
Wing chord (min)	5.1 ft
Wingspan	118.2 ft
Wing Leading Edge Sweep Angle	24 deg
Fuselage Length	106 ft
Fuselage Width	17.2 ft
Fuselage Height	12.4 ft

Several assumptions and aspects of the design process are relevant to noise and so will be highlighted here. The baseline engine architecture of the ND8 calls for dual two-spool geared turbofan engines mounted within the tail structure at the aft dorsal location on the fuselage. It is noted here that this configuration is a departure from the MIT/Aurora D8, which features a reverse-flow core that is mechanically linked to the fan through a gearbox [4]. The reverse-flow core design is necessary to satisfy the rules set by the FAA to minimize risk that fragments ejected from an uncontained engine failure could cause excessive harm to other critical systems, such as the other engine or flight control surfaces [26]. Since the ND8 is a technology collector for AATT, and is not intended to meet all FAA airworthiness certification criteria, the engines are mounted in this way for the present analysis. An important aspect of the engine design relates to the physical size constraints of the geared turbofan engines. The ND8 features a ‘pi-tail’ with dual vertical stabilizers bridged at the top by a horizontal stabilizer. Because the ND8 configuration dictates that the engines are placed within the pi-tail, the maximum fan diameter is limited to 1.82 m (72 inches). To meet climb performance metrics, the fan

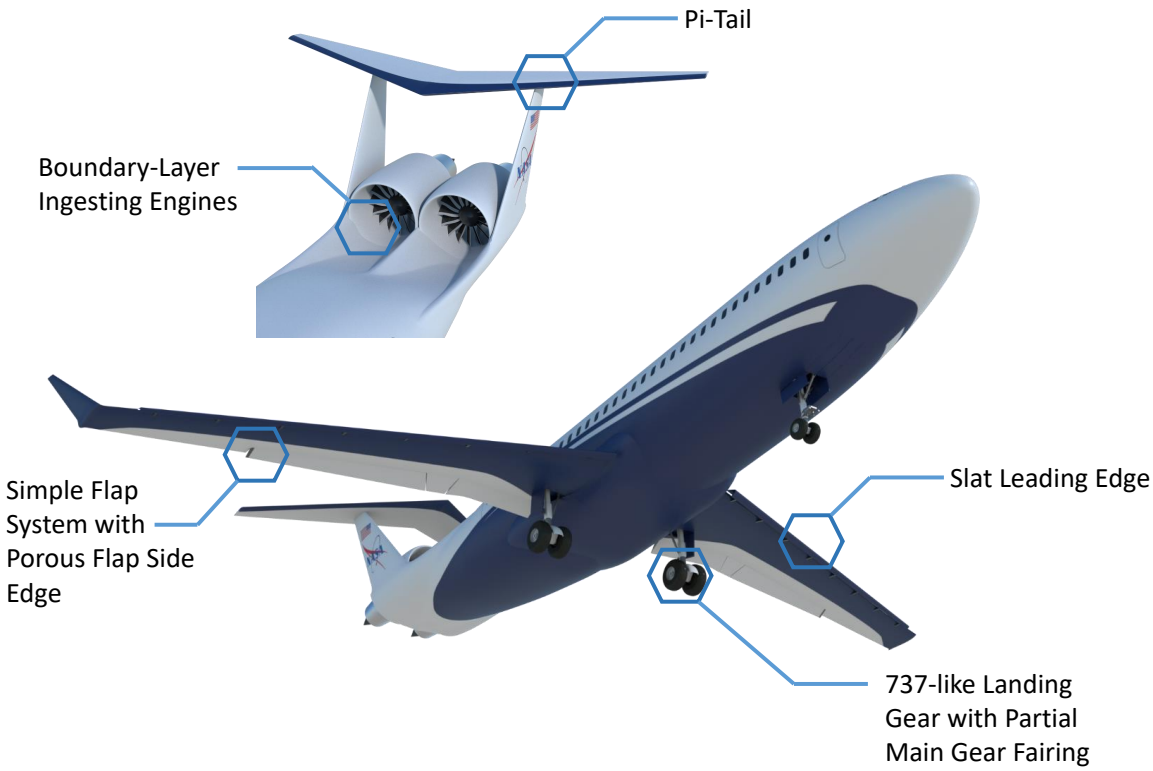

Fig. 4 Design elements of the ND8 concept, with closeup view of tail section (inset).

pressure ratio (FPR) is designed to provide enough thrust for a given fan diameter. The engine core is constrained to a minimum size, which reflects the expected physical limitations of core technology in the 2035 time frame [7]. The final design of the ND8 engine calls for a fan pressure ratio of 1.35 and a bypass ratio of 16 at takeoff conditions. This design is beyond the current state-of-the-art engines with maximum bypass ratios around 11 for this size class, but significantly less aggressive than the geared turbofan engines designed for other advanced aircraft concepts with bypass ratios around 25 [20, 22, 27]. Other aspects of the ND8 engine are given in Table 2 and compared to a similar engine-under-wing aircraft from ERA [22], the 160-passenger tube-and-wing aircraft (TW160). Key differences include the lower bypass ratio and higher tip speed of the ND8 engine, which lead to higher noise source levels. Multidegree-of-freedom (MDOF) acoustic liners are applied to the ND8 engine using the specified duct length and height from the NPSS engine definition. An interstage liner is included with an effectiveness of 50%, consistent with prior studies [27]. The effects of soft vane liner technology along with sweep and lean of the stator vanes are included in the modeling of fan noise.

The high-lift system of the ND8 consists of a conventional slat leading edge device and a single element flap trailing edge device. The trailing edge flap configuration minimizes discontinuities between flap elements, a design characteristic featured on modern commercial airliners. This leads to a significant reduction in flap-side-edge noise compared to

Table 2 ND8 engine parameters and takeoff (TO) conditions compared to the TW160 engine from the ERA Project [22].

	ND8	TW160
Fan diameter (ft)	5.9	7.0
Number of fan blades	18	18
Number of fan stator vanes	40	40
Normalized rotor-stator spacing	1.52	1.52
Fan pressure ratio at TO	1.35	1.23
Bypass ratio at TO	16.0	25.5
Net thrust at TO (lb)	15,900	16,700
Fan RPM at TO	3670	2640
Fan tip Mach at TO	1.02	0.88
Aft duct liner length-to-height ratio (L/H)	1.95	1.83
Inlet duct liner length-to-radius ratio (L/R)	0.96	0.68
Interstage liner effective L/H	0.34	0.27

the reference aircraft (Boeing 737-800). In addition, the effect of porous flap side edge Mid Term technology [28] is included in flap noise modeling, consistent with prior studies [20]. Flight-condition-specific parameters for the high-lift system (flap deflection angles, etc.) are used for noise predictions at each stage of flight. The landing gear consist of a 737-type tricycle gear system with two wheels per main gear and nose gear. A partial main gear fairing Mid Term technology [28, 29] is included in the modeling of main gear noise, consistent with prior studies [20].

The flight profile plays a critical role in setting certification noise levels since Mach number and angle of attack determine airframe noise source levels, and the flight path controls noise propagation distance to observers. Takeoff flight path information for the ND8 and two other aircraft, the TW160 and a NASA-modeled 737-800-like aircraft, are shown in Figure 5, and additional parameters are given in Table 3. The reduced thrust requirements at cruise due to boundary layer ingestion lead to reduced climb performance at takeoff compared to the reference aircraft. As a result, the ND8 is projected to reach an altitude 100 feet lower than a 737-like aircraft at the cutback certification point (21,325 feet downrange of brake release). This small difference is expected to have a minimal impact on certification noise, but is a departure from other concept aircraft of a similar size, which are expected to climb nearly 200 feet above the 737-like aircraft at the cutback point [27]. Aircraft speed at each of the three points also plays a role in total certification noise. The slower speed of the ND8 compared with other aircraft may lead to reduced source noise of airframe components, but is unlikely to have an effect on engine noise source levels. In fact, a slower flight speed is detrimental if the aircraft is engine-noise dominant, as slower speeds lead to longer integration times in the EPNL calculation.

IV. ND8 PAA Effects

The majority of features on the ND8 will be predicted using the methods available in ANOPP-Research as described in Section II. However, there are several unique features of the ND8 that require special attention along with the

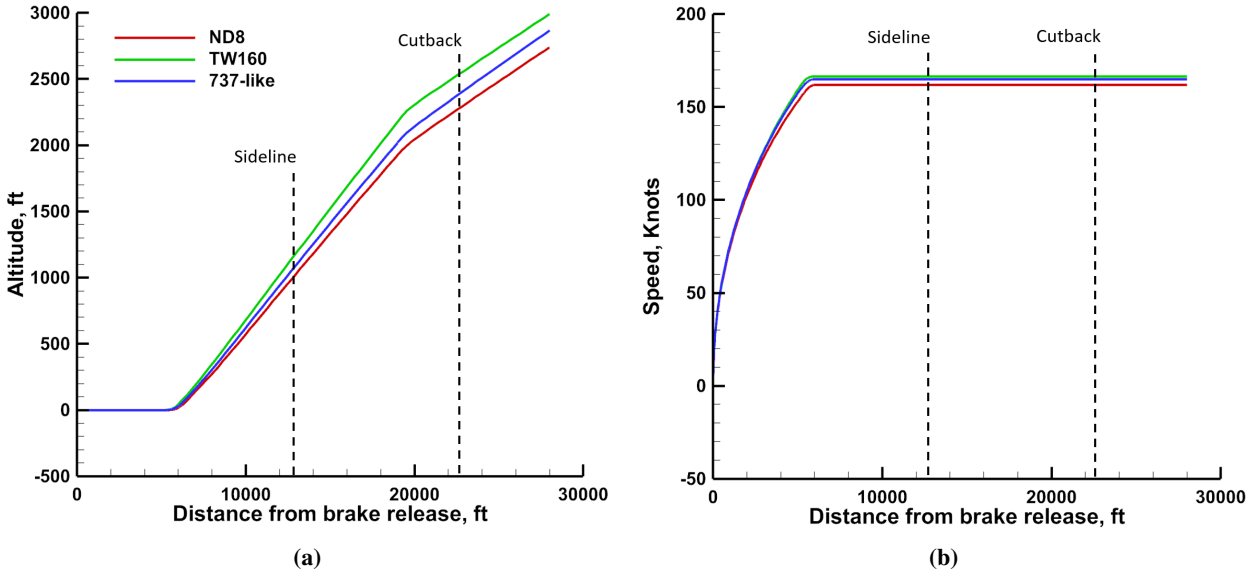

Fig. 5 a) Flight path and b) calibrated airspeed schedule of the ND8, TW160, and 737-like aircraft.

Table 3 ND8 flight path parameters compared to those of the TW160 and 737-like aircraft.

		Climb Angle (deg)	Angle of Attack (deg)	Thrust Fraction	Speed (knots)
Approach	ND8	-3.0	7.7	0.17	145
	TW160	-3.0	6.1	0.19	149
	737-like	-3.0	6.5	0.12	149
Sideline	ND8	8.6	6.8	1.00	162
	TW160	9.5	6.6	1.00	167
	737-like	9.0	6.9	1.00	165
Cutback	ND8	5.0	7.4	0.75	162
	TW160	4.9	7.3	0.68	167
	737-like	5.3	7.6	0.76	165

development of new methods to reasonably predict the flight noise at a system level. The first feature is boundary layer ingestion, which describes the inflow of slow-moving, turbulent air close to the fuselage into the engine that results in unsteady fan blade loading and increased fan noise. The second feature is the placement of the engines on top and at the rear of the fuselage within the pi-tail, which leads to engine noise shielding by the fuselage and vertical stabilizers, but potential noise reflections by the horizontal stabilizer along with diffraction around the edges of the airframe. The methodology for treating each of these features is now described. To develop a noise model for boundary layer ingestion, three options were identified to predict the effect on fan noise. The use of analytical, numerical, and empirical tools were all considered.

A. Boundary Layer Ingestion Modeling

Analytical methods have been developed to describe the aeroacoustic effects of turbulence ingestion into rotors and fans. Majumdar and Peake [30] provide a theoretical model for the effect of turbulence ingestion into a fan, and results are given for the ingestion of atmospheric turbulence at static and flight conditions. Further use of this theory would require knowledge of the ingested turbulent velocity spectrum. The theory of Glegg et al. [31] is a time-domain approach, which eliminates modeling of the turbulence spectrum, but requires measurements of the four-dimensional inhomogeneous velocity correlation function. For the present study, it was determined that the lack of detailed flow field information prevented the use of rigorous analytical methods.

Numerical methods have the potential to capture the relevant physics to reasonably predict BLI noise. Envia [32] describes a simulation that uses 3D linearized Euler analysis to calculate the acoustic transmission of tonal noise through a fan. The simulation was performed using the NASA code LINFLUX [33]. For the study, the source of the tonal noise was the interaction between the wakes of the fan rotor blades with the outlet guide vanes (OGVs) of the NASA/Pratt and Whitney 22-inch Advanced Ducted Propulsor (ADP). The Euler model was a general inviscid formulation of the interaction between vortical, acoustic, or entropic perturbations with a row of turbomachinery blades. The computational methodology treated the problem in two separate steps. First the acoustic response of the OGV to the rotor wake was computed. Then, the model was used to predict the transmission of the resulting acoustic field through the rotor blades. Simulation results showed good agreement with experimental noise measurements, and clearly identified the need to account for rotor interactions when tracking tonal noise from the OGVs.

This simulation toolset LINFLUX provides a framework by which boundary layer ingestion could be modeled by direct input of the expected distortion field. Although the capability was designed particularly for rotor/stator interaction, the inflow distortion could be thought of as coming from some object upstream of the rotor. By directly defining the Fourier coefficients of the distortion field, the model can calculate the response of the moving rotor blades as it does with the OGVs of the previous study. The acoustic field would then be propagated upstream and to the surrounding domain to determine far field noise. This methodology was considered as a strong candidate to predict BLI noise, but the significant time required in both setting up and running the simulation, along with the lack of information on the expected distortion field, meant that this would require a dedicated study of its own, and so remains for future work.

To the authors' knowledge, a comprehensive experiment in which noise is measured from a turbofan ingesting a thick (~100% blade span [8]) turbulent boundary layer has not been performed. As analytical and numerical methods have been ruled out from this investigation, the most promising way forward is to consider the physics of boundary layer ingestion, break down the phenomenon into its constituent components, and define the acoustic effect of each component using data from relevant experiments. This process is shown in conceptual form in Figure 6. The overall physics of boundary layer ingestion is broken up into two parts - the ingestion of turbulence into the fan face, and the once-per-revolution change in angle of attack of the fan blades due to the decreased mean flow velocity entering the

lower portion of the engine inlet. Turbulence ingestion is expected to have both a broadband and tonal effect on fan

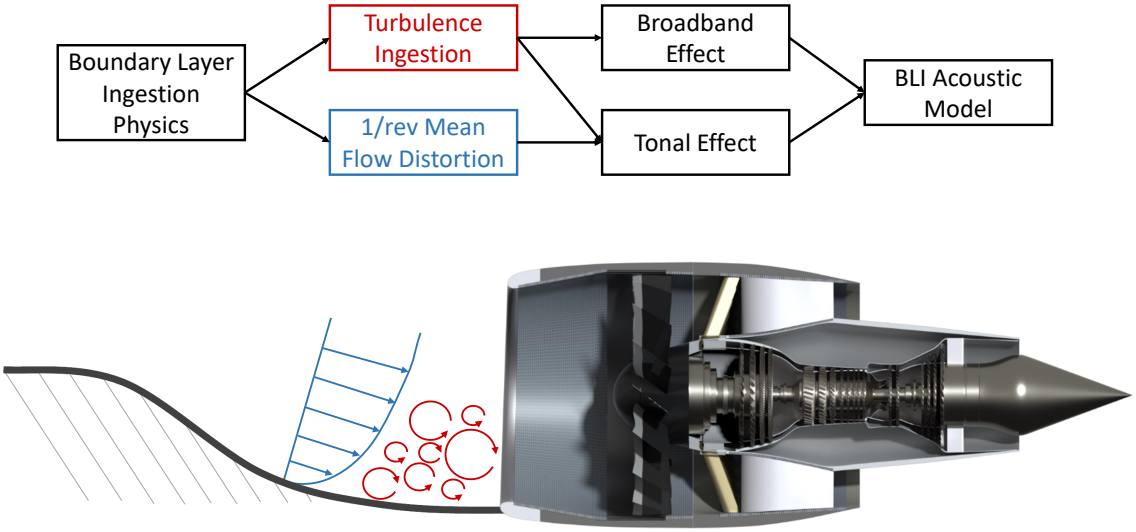

Fig. 6 Acoustic modeling process for boundary layer ingestion, and artist rendering of the ND8 engine with upstream boundary layer.

noise. The broadband effect is expected due to the unsteady random nature of boundary layer turbulence, while the tonal component arises because this turbulence can be stretched as it is drawn into the engine and cut multiple times by successive fan blades leading to tones at the blade passage frequency and harmonics. The change in blade incidence angle is expected to have only a tonal effect, as the fan blades experience a change in loading over regular intervals as they pass through the region of slower-moving fluid. Combining these effects leads to a BLI model that can be applied to fan noise.

1. Turbulence Ingestion

Turbulence ingestion has been a subject of active research for many years. One of the first breakthrough studies was published by Hanson [34], wherein it was found that the additional noise observed in static engine tests was due to the ingestion of stretched atmospheric turbulence. This led to the development of inflow control devices (ICDs) for static engine tests. The ICD's serve to smooth the airflow entering the engine inlet and remove much of the ambient vorticity and turbulence present in the atmosphere that may be stretched and intensified during the test. During the development of these devices, many acoustic experiments were performed which measured noise from static engines with and without ICDs in order to quantify their effectiveness. These experiments provide a useful database of noise measurements with and without turbulence ingestion from which an acoustic model can be built.

Jones et al. [35] describe noise measurements of a static JT15D engine mated with two separate ICD designs - one

internal to the engine inlet, and one external. Their results showed that both ICDs led to significantly smoother inflow indicated by a sharp reduction in blade-passage frequency (BPF) tones. However, the internal ICD was seen to alter the acoustic propagation behavior of the inlet duct, while the external ICD was largely acoustically transparent. This was determined by placing rods in the inlet to create flow distortions and strong BPF tones which would dominate those from any natural atmospheric inflow distortion. The addition of rods to the inlet led to increases in BPF tones of up to 15 dB, which propagated cleanly through the external ICD but were attenuated by the internal ICD. Without rods, the external ICD was observed to reduce the BPF tone level by up to 10 dB over a wide range of polar angles due to the removal of inflow distortions caused by atmospheric turbulence.

Preisser and Chestnutt [13] describe flight tests of a JT15D meant to eliminate all effects of inflow distortion and to compare with earlier results. The engine was attached to a Grumman OV-1 aircraft and flown past a series of 30-ft pole microphones. Their results indicated that the inflow control devices tested previously led to a good representation of the measured BPF levels in flight. They also present results for broadband noise levels at static conditions and in flight, taken as the spectral level at the base of the BPF peaks. They show a significant influence of inflow distortion on broadband noise, up to 6 dB across a wide range of polar angles. This study represents the best comparison of results from this project, and so greatly informs the turbulence ingestion model for the present study.

The results of Preisser and Chestnutt for a static fan with subsonic blade tip speeds with and without an ICD, along with the results of Jones et al. [35] and supplementary flight test results [36] have been used to build a general prediction of this effect on the blade passage frequency tone as shown in Figure 7a. Most of the noise from turbulence ingestion is radiated at a ninety degree angle to the inlet direction, which corresponds to the nearest point of an aircraft flyover, and so is likely to strongly influence system noise. The results of Preisser and Chestnutt are also used to build a prediction of the effect of turbulence ingestion on broadband noise, as seen in Figure 7b. In contrast to the tonal noise, the broadband noise is seen to radiate primarily in the upstream and downstream directions. The deltas shown in Figure 7 are added to the fan source noise levels computed by the models in ANOPP that are described in Section II.

With these models in hand, it is useful to compare with other experiments, certain aspects of which make their results unsuitable for model development, but which may still serve as qualitative and order-of-magnitude quantitative checks on the general aspects of the model. Clark et al. [37] tested a 10% scale model of the Pratt and Whitney Advanced Ducted Propeller (ADP) with several inlet shapes (short, long, scarfed, and elliptical) in the NASA Langley 14- by 22-Foot Subsonic Tunnel. The different inlet shapes caused nonuniformity of the inlet boundary layer thickness that led to unsteady forces on the fan that propagated as increased fan noise over the entire acoustic measurement region. Spatially integrated sound pressure levels (SPL) indicated that the variation in boundary layer thickness dominated over any noise benefit obtained from varying the inlet shape, and that even small changes in boundary layer thickness resulted in increased tonal levels for the 1-, 2-, and 3-BPF tones of up to 7 dB. Considering the maximum change in boundary layer thickness for this test was between 1.5 and 4.2% blade span, compared with the nearly 100% blade span

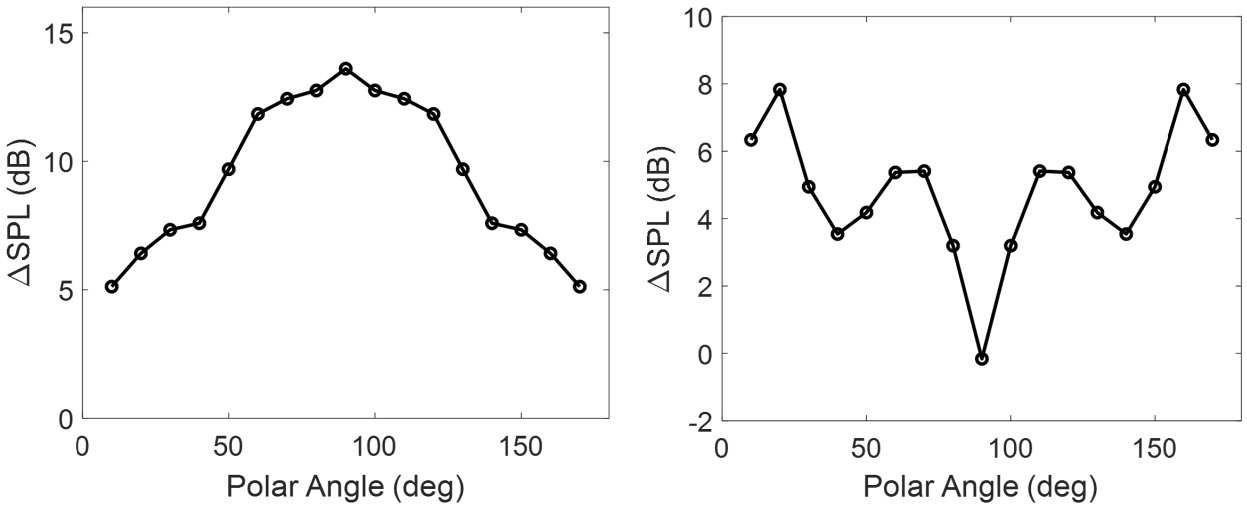

Fig. 7 Acoustic model for the a) tonal and b) broadband effect of turbulence ingestion.

boundary layer thickness expected for the ND8 with BLI, the relative magnitude of the model for the present study is considered reasonable.

Koch [38] conducted a series of studies using the Advanced Noise Control Fan (ANCF) at the NASA Glenn Research Center. Several configurations of cylindrical rods were placed just upstream of the fan to produce a distortion pattern over the fan face. Acoustic measurements were made in the anechoic test facility surrounding the static fan rig, and the results indicated an increase in both tonal and broadband noise. Measured tonal levels increased by 20-25 dB nearly symmetrically upstream and downstream of the fan, while broadband levels increased by about 7 dB. The fan used in this experiment was a low-speed, low-pressure-ratio fan with physics unlike those expected for a true turbofan, which may explain the difference in the directivity pattern between this case and the present model. Due to the difference in fan characteristics, these data were not used in generating the model for the present study, but nonetheless serve as a check for the relative magnitudes expected for high levels of inflow distortion. The relative magnitudes of predicted noise levels for the present study are consistent with the observations of Koch [38].

2. Mean Flow Distortion

The boundary layer developing over the fuselage leads to a region of low-momentum inflow over the lower portion of the fan face. This leads to a once-per-revolution change in incidence angle of the blades as they move through this low-axial-speed region of flow. This change in incidence angle leads to strong unsteady blade loading, which presents acoustically as strong tones at the blade passage frequency and harmonics. Few experiments have been performed which feature this velocity deficit in a fan's inflow, and none are known to include noise measurements. However, if the change in incidence angle over rotation is the focus, an analogous situation is one in which an open rotor is placed at an angle of

attack relative to the incoming flow. Geometrically, this creates an angle of attack difference as the advancing blades see a change in inflow relative to the receding blades.

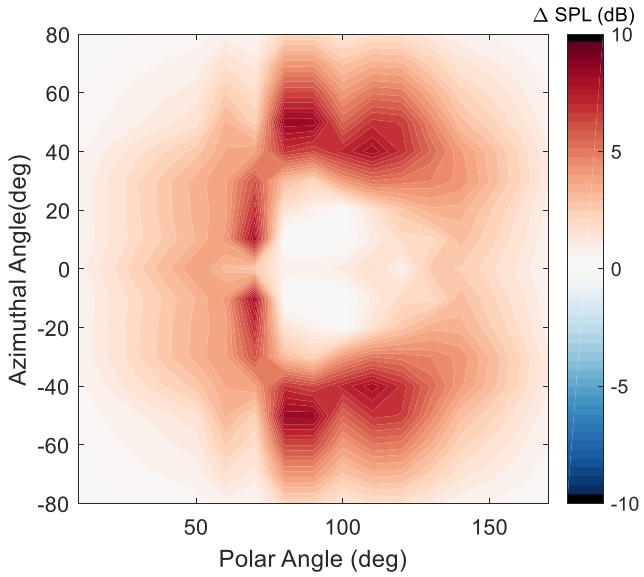

Fig. 8 Acoustic model for the tonal effect of a once-per-revolution change in fan blade incidence angle.

Czech and Thomas [39] tested a counterrotating open rotor in the Boeing Low Speed Aeroacoustic Facility. Among other tests, the rotor was placed at angles of attack of 0, 7, 10, and 13 degrees relative to the incoming flow. At 10 degrees angle of attack, using the blade geometry, flow conditions, and rotational speed of the open rotor, simple geometric calculations indicate that the change in incidence angle of the blades at 70% span is approximately 4 degrees, which is less than that expected for the ND8 with BLI. However, the data used here represent the best-available information on this effect. Acoustic data are available for a wide range of polar and azimuthal angles, which can be used to build an acoustic model. The forward rotor BPF tonal levels are extracted from all angle of attack cases. The zero angle of attack result is subtracted from those of the nonzero angle of attack cases, and the resulting changes in level are averaged to yield a general prediction model for the mean flow distortion effect on the BPF tone shown in Figure 8. It can be seen that this type of effect has the highest influence along the sideline direction.

For the current investigation, the two BLI effects (turbulence ingestion and mean flow distortion) are assumed to be decoupled, which permits the simple summation of the noise models. Once the two tonal effects are summed, the result is a function of both polar and azimuthal angle. The values here were chosen such that they apply to the fundamental BPF tone. To model the higher harmonics (up to 4BPF), the noise levels are subtracted by 3 dB for each harmonic to model a decreasing effect of BLI with increasing BPF harmonic. Limited data from Jones et al. [35], Clark et al. [37], and Koch [38] suggest that higher harmonics are affected by nearly the same amount as the fundamental tone, but the use of a 3 dB subtraction for each harmonic represents a conservative choice to predict this effect.

B. Noise Shielding, Reflection, and Diffraction

The noise scattering effects (shielding, reflection, and diffraction) of the ND8 present a special challenge for system noise modeling. Several features of the ND8 aircraft must be considered to develop a comprehensive model of the engine noise scattering effects. Most evidently, the fuselage structure in front of and below the engines will provide the majority of shielding to the engine inlet at low azimuthal angles (near the flyover plane) and in the forward direction. Importantly, the aft fan nozzles are integrated into the trailing edge of the fuselage and are entirely unshielded, as seen in Figure 9. Just upstream of the engine nacelles, the upper fuselage surface forms two "scoops" which serve to guide the boundary layer flow into the engines. The scoops provide some shielding benefit, particularly at sideline angles. On the MIT/Aurora D8 [4], the leading edges of the vertical stabilizers are placed far upstream of the engine inlets, providing a strong noise benefit at sideline. However, this is not true for the ND8 due to a combination of different vertical tail sizes, engine positions, and inlet lengths, which arise from the different modeling assumptions of NASA and MIT/Aurora. As a result, the leading edges are directly adjacent to the engine inlets, as seen in the inset in Figure 4, such that the vertical stabilizers do not provide any shielding benefit. The horizontal stabilizer is placed above and slightly downstream of the engines. This provides a reflecting surface for engine noise to be radiated at aft angles. The spanwise extent of the horizontal stabilizer dictates the level of reflection in the sideline directions.

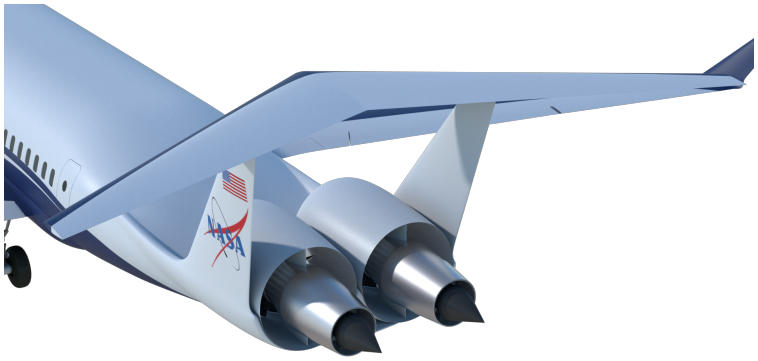

Fig. 9 Closeup rear view of the ND8 tail section. Aft-radiated fan noise is entirely unshielded due to the integration of the fan nacelle with the rear fuselage structure.

Several experiments have been carried out to quantify acoustic shielding by some airframe configurations, most notably the hybrid wing-body (HWB). PAA experiments by Czech et al. [40] were performed in the Boeing Low Speed Aeroacoustic Facility (LSAF). This experiment featured a broadband noise source inside a nacelle placed at various locations near a hybrid wing-body airframe at flow conditions representative of takeoff and approach, with acoustic measurements taken at a wide range of polar and azimuthal angles to quantify the shielding effects of the airframe. The data from these experiments, including many datasets not described in the publications, are used to develop noise shielding maps. Through a unique data processing algorithm, data from these tests are scaled and mapped appropriately to reflect the unique geometric features of the ND8 airframe. As these data are obtained from experiment, they include

all effects of shielding and diffraction. Figure 10 shows the results of this process for a single frequency (1 kHz). Shielding of inlet noise by the fuselage is the most prominent feature. Some sideline shielding by the engine scoops is visible, and the reduced levels here reflect the fact that the relatively small, thin scoops will be less effective shields than the full fuselage, and fan noise will diffract around the edges to the sideline angles. Reflection effects are added analytically by computing the specular reflection angles of the engine noise off the pi-tail. Some amplitude loss due to reflection is assumed in the process. These results are applied to both fan noise and core noise, as the locations of these two sources lead to similar shielding characteristics.

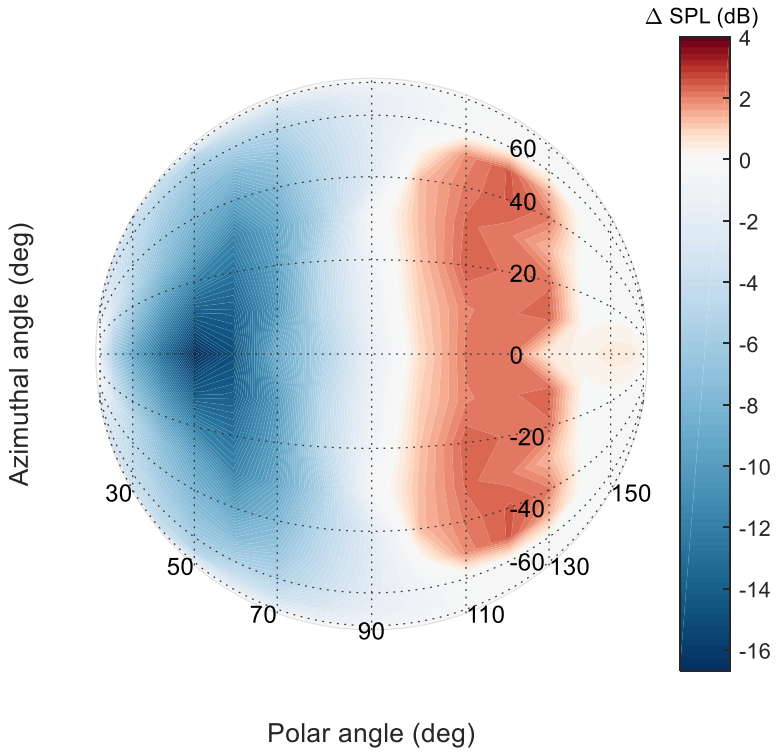

Fig. 10 Scattering effects of the ND8 engine noise by the airframe at 1 kHz.

V. Mid Term Aircraft - Results and Discussion

With the methodologies and tools described in previous sections, the noise metrics for the ND8 are calculated and shown in Table 4. The noise of the ND8 was computed with various combinations of boundary layer ingestion and scattering effects included in order to quantify each effect. Results are given as margins to Stage 4 certification levels for consistency with prior publications, as well as published NASA goals. The "baseline" ND8 is first presented. The noise of this nonphysical aircraft is computed assuming no PAA effects (no scattering and no BLI). From here, scattering

effects are added. Following this, the broadband and tonal BLI effects are added separately to quantify the system-level impact of each individual component. Next, scattering effects are removed and all BLI effects are included. Finally, all PAA effects are combined into a complete prediction of the ND8 aircraft.

Table 4 Certification levels (EPNdB) for each ND8 configuration.

PAA Effects Included	Approach	Sideline	Cutback	Cumulative	Margin to Stage 4	Noise Increase from Baseline
None (Baseline)	86.4	86.7	81.5	254.6	22.3	-
Scattering	85.0	85.9	81.6	252.5	24.5	-2.1
Scattering and Broadband BLI	86.8	88.7	84.8	260.3	16.6	5.7
Scattering and Tonal BLI	86.8	91.3	86.4	264.5	12.4	9.9
All BLI	89.9	93.1	87.6	270.6	6.3	16.0
All PAA	88.0	92.1	87.4	267.5	9.4	12.9

Considering first the ND8 with no PAA effects, the cumulative margin to Stage 4 is 22.3 EPNdB. When scattering effects are added, the margin increases to 24.5 EPNdB. Most of this benefit is obtained at the approach certification point, where forward-radiated fan noise plays the most significant role. At sideline, reduced shielding leads to less of an impact on EPNL levels. At cutback, lack of aft shielding and the dominance of aft-radiated fan noise, together with reflections from the tail, cancel out the benefit of forward shielding. When BLI effects are included, noise levels are drastically increased due to the increase in both forward- and aft-radiated fan noise. With both broadband and tonal effects included, levels are increased 16.0 EPNdB above the baseline configuration. Shielding of the forward-radiated fan noise moderates this increase by 3.1 EPNdB, again having most influence at approach, leading to a final cumulative margin to Stage 4 of 9.4 EPNdB.

With scattering effects held constant, the tonal BLI effect is seen to have nearly twice the influence as the broadband BLI effect. This is because of the greater magnitude of tonal levels predicted for BLI, in addition to the fact that increased tonal levels have a two-fold effect on computed EPNL. Not only do greater tones increase the absolute magnitude of the received noise, but they also increase the computed tone penalty of the tone-corrected perceived noise level, which is then integrated to obtain EPNL. The effect of BLI on tones was modeled based on the BPF harmonics of the fan, which is dependent on operating condition (fan RPM). At sideline (full throttle setting), the BPF tone is placed in the 1-kHz one-third-octave band, with the higher harmonics affected by BLI placed in the 2-, 3-, and 4-kHz bands. The frequency range from 2- to 4-kHz is the highest-weighted frequency range for calculating perceived noise level. As a result, the greater tones here are particularly effective at increasing EPNL. At cutback, the tones are slightly reduced in frequency, but only at the approach condition do the first three harmonics fall below 2 kHz. This leads to reduced influence of BLI on approach certification levels - with scattering effects held constant, the complete BLI effect yields a 3.0 EPNdB increase, compared to 6.2 EPNdB and 5.8 EPNdB increases at sideline and cutback, respectively.

Figures 11 through 13 show tone-corrected perceived noise levels with and without BLI effects at each of the three

certification points. Several key observations can be extracted from these plots that lead to greater understanding of the ND8 noise characteristics. The first observation is the clear dominance of fan noise at all certification points, even when no BLI effects are included. This shows that fan noise is the primary driver of EPNL. The situation is only made worse by the BLI effects, which lead to such a high dominance of fan noise that other noise sources contribute almost nothing to overall EPNL levels. It is thus apparent that the feasibility of the ND8 as a quiet aircraft is first dependent on the control of BLI noise, followed by additional modifications to further reduce fan noise. It is anticipated that the noise penalty associated with BLI could be controlled through careful design of the propulsion system. For example, a boundary layer suction system could remove much of the flow distortion, leading to a smoother flow into the fan. Such a system would only be used near the ground, as its use would negate the expected fuel burn benefit associated with boundary layer ingestion.

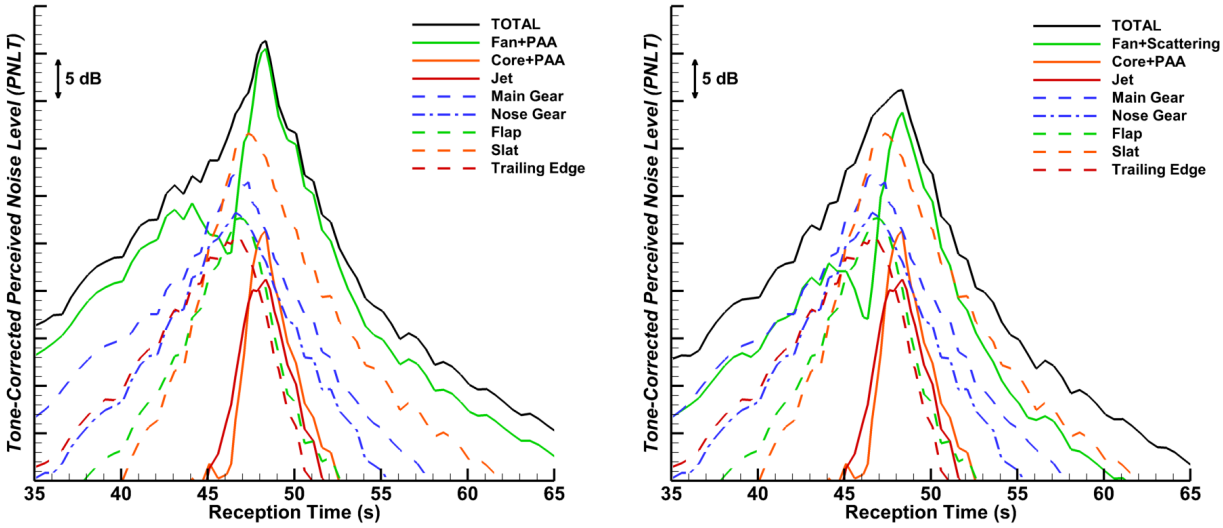

(a) All PAA effects included. **(b) Acoustic BLI effect suppressed.**

Fig. 11 ND8 source levels calculated over reception time as the aircraft flies past the approach certification point.

Assuming the inflow distortion could be controlled, it is useful to examine the PNLT plots without boundary layer ingestion to gain further insight into how noise could be further reduced. Considering first the approach levels in Fig. 11, the influence of forward shielding by the fuselage is immediately apparent. As fan noise is reduced in the forward arc, airframe sources therefore contribute significantly to EPNL. In particular, the flap, slat, and main gear are all seen to have similar noise levels that are higher than fan noise until the lack of aft shielding again leads to dominance of fan noise. Nose gear, jet, core, and trailing edge noise are insignificant here. At the sideline (Fig. 12) condition, jet and fan noise play a nearly equal role in determining EPNL levels without the acoustic effect of BLI. These noise sources could be reduced by utilizing a higher bypass ratio engine, but this would require modification of the pi-tail to eliminate the fan diameter constraint. This modification could lead to further fan noise reduction if the vertical stabilizers could be

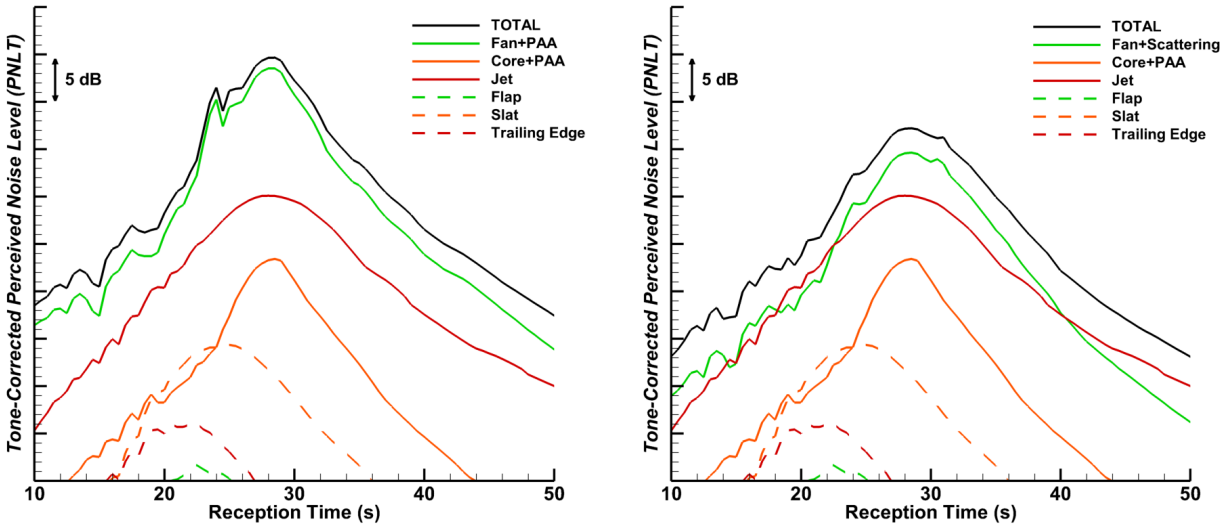

(a) All PAA effects included. **(b) Acoustic BLI effect suppressed.**

Fig. 12 ND8 source levels calculated over reception time as the aircraft flies past the sideline certification point.

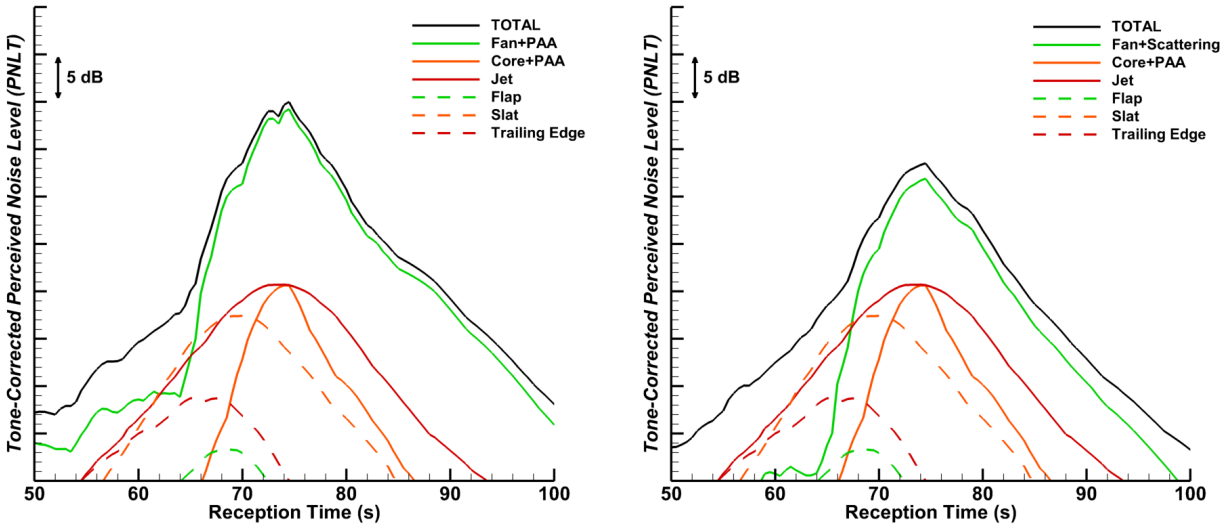

(a) All PAA effects included. **(b) Acoustic BLI effect suppressed.**

Fig. 13 ND8 source levels calculated over reception time as the aircraft flies past the cutback certification point.

altered to provide more sideline shielding. Finally, at cutback (Fig. 13), fan noise peaks at a level approximately 11 dB above jet noise. Dominance of aft-radiated fan noise, along with reflections by the pi-tail, are the primary factors contributing to cutback EPNL. Few options are available to increase aft-radiated fan noise shielding, but modifications to the pi-tail could reduce or eliminate reflections.

Even if inflow distortion is well controlled such that BLI noise is eliminated, the ND8's cumulative margin to Stage 4 of only 24.5 EPNdB falls well short of the NASA Mid Term goal of 32-42 EPNdB. As a final point of comparison, the equivalent Mid Term TW160 concept was predicted, using a similar methodology as described here for the ND8, to

reach a margin to Stage 4 of 28.5 EPNdB. The decreased bypass ratio of the ND8 is expected to be responsible for the majority of the difference, as this leads to a supersonic fan tip Mach number at sideline, compared to the subsonic fan tip Mach number of the larger TW160 engine. The lower bypass ratio of the ND8, together with the dominance of aft-radiated fan noise, reduced climb performance, and similar PAA effects (aft reflections from the tail and wing for the ND8 and TW160, respectively), lead to higher noise levels than the TW160. For the ND8 to reach NASA Mid Term goals, the tail section must be redesigned to accommodate higher bypass ratio engines and to provide more side and aft shielding, although a redesign of this magnitude may be incompatible with the boundary layer ingestion feature that is critical to the fuel burn goal. It is expected that multidisciplinary design and analysis may be necessary to determine if a future iteration of the ND8 could be a viable candidate to meet the NASA Mid Term goals for fuel burn and noise simultaneously.

VI. Far Term Noise Reduction Technologies

As mentioned in Section III, the Mid Term noise assessment of the ND8 included Mid Term level technologies. Multiple-degree-of-freedom acoustic liners are applied to all engines using the specified duct length (L) and height (H) from the NPSS engine definition. An interstage liner is also included. The effects of soft vane liner technology along with sweep and lean of the stator vanes are included in the modeling of fan noise. The effect of porous flap side edge technology [28] is included in flap noise modeling. Finally, a partial main gear fairing [28, 29] is included in the modeling of main gear noise. All implementations of noise reduction technologies are consistent with prior studies [20, 27, 41]. In order to evaluate NASA's noise reduction technology portfolio and determine the ND8's Far Term noise potential, more advanced Far Term noise reduction technologies (listed in Table 5 and described below) will be incrementally added, and system-level noise predictions will be repeated after each addition. In cases where two technologies are incompatible and/or overlapping (for example, partial main gear fairing and pod gear), the effect of the earlier technology will be removed prior to adding the more advanced one. As with the Mid Term technologies, only the acoustic effect of each technology will be considered; the impact of each technology on performance or operating condition of the aircraft, if any, is not incorporated into the prediction process.

As in the baseline assessment, two versions of the ND8 will be carried forward throughout this roadmap. The two versions are differentiated by whether or not the acoustic effects of BLI are included in the noise prediction. Because of the large 15 EPNdB cumulative penalty associated with BLI, a boundary layer diverter or active flow control system would be a desirable design feature to be used at community noise conditions (approach and departure). Such a system could then be deactivated at cruise in order to take advantage of the expected fuel savings associated with BLI. However, such a system is likely to be complex and heavy, such that further design work and trade studies must be undertaken to determine whether the advantages of such a system outweigh the costs. Therefore, both scenarios are considered through this roadmap to further inform this future decision in terms of the expected acoustic benefit.

Table 5 Complete list of all Far Term noise reduction technologies applied to the ND8.

Technology	Noise Component
Bifurcation Liner	Aft Fan
Over-the-Rotor Treatment	Fan
PAA Liner	Aft Fan Reflection
Scarf Nozzle	Aft Fan
Lip Liner	Forward Fan
Center Plug Liner	Core
Slat Cove Filler	Leading Edge
Sealed Slat Gap	Leading Edge
Continuous Moldline Link Flap	Flap Side Edge
Pod Gear	Main Gear
Nose Gear Fairing	Nose Gear

A. Engine and PAA Technologies

Several Far Term technologies in the AATT portfolio are focused on reducing fan noise, which is a dominant noise source on the ND8. A selection of technologies is shown in Figure 14. First, acoustic liners will be added to the engine bifurcation structure. In previous work [27, 42], bifurcation liners were not added due to the relatively thin bifurcations found in the smaller engines of single-aisle class aircraft. However, discussions with subject matter experts have led to the conclusion that the addition of liners would require thickening the bifurcation by only a few inches, which is acceptable within the framework of this study. The addition of bifurcation liners will impact the fan noise radiated in the aft direction, precisely the region that will have the maximum impact on system level EPNL. The effect of the bifurcation liner is modeled in ANOPP-Research through an effective increase in the quantity *L/H* of the aft duct, which determines the magnitude of noise attenuation achieved by the aft duct liner. The frequency range of attenuation is not modified by the bifurcation liner. This is equivalent to adding additional lined area to the aft duct, and no attempt is made to model the unique effects of placing the lined area on the bifurcation itself. To further reduce fan noise, an over-the-rotor acoustic liner (placed in the rub strip area around the fan) will be incorporated into the fan noise prediction. Over-the-rotor liners have had successful proof-of-concept demonstrations [43, 44], and offer potential for fan noise reduction across a wide range of directivity angles. Data from these preliminary experiments are used to determine a relative reduction in fan noise for use in ANOPP.

The ND8 features unfavorable PAA effects related to reflections from the pi-tail. These effects can be mitigated through the use of PAA liner technology, which is implemented as an acoustic liner embedded in the lower surface of the horizontal stabilizer. A similar PAA liner has been demonstrated in a successful proof-of-concept experiment with a counterrotating open rotor propulsion noise source with the effects of forward flight [39]. The development of lower drag facesheets for acoustic liners [45–48] aids the practical implementation of this technology. The effect of PAA liners is modeled through a modification of the computed PAA effects discussed in Section III. The magnitude

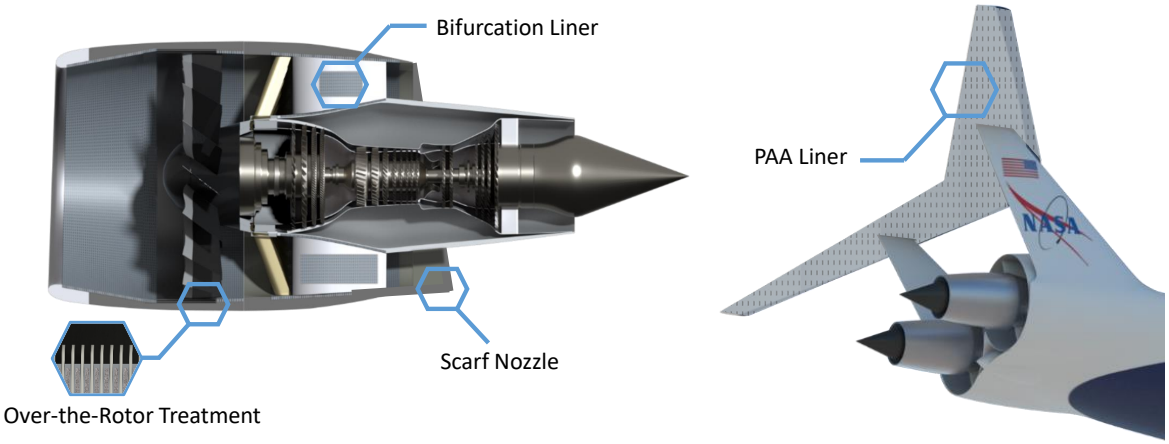

Fig. 14 Artist renderings of the noise reduction technologies applied to the ND8 engine and aft section.

of reflections from the main wing or pi-tail are reduced by a factor of 2 (on a pressure-squared basis) in the angular regions corresponding to placement of PAA liners for maximum impact on community noise. The liners are expected to be effective over a frequency range of 1-2 kHz, which is both important for EPNL calculation as well as inclusive of prominent BPF harmonic tones.

A negative scarf is incorporated into the fan exit nozzle in order to increase the aft-shielding of fan noise. The negative scarf lengthens the bottom of the fan nozzle relative to the top, leading to reflection of fan noise away from ground observers. As this leads to a fan noise reduction in overhead and mild aft angles, this could have a significant impact on system level noise. The acoustic effect of the scarf nozzle is determined using unpublished experimental data from a wind tunnel test campaign jointly conducted by Boeing and NASA in Boeing's LSAF [49]. As part of that campaign, a broadband noise simulator was placed inside two different engine nacelle simulators, one with a scarf nozzle and one without. The effects of forward flight were included. Far-field acoustic data from that experiment form the basis of the scarf nozzle model implemented in ANOPP.

To reduce inlet-radiated fan noise, an inlet lip liner is applied by extending the effective length of the inlet liner to the full length of the inlet, where normally the inlet liner would be assumed to extend only from the fan casing to the throat. This technology has been tested previously [50] with promising results. The lip liner is seen as an important technology to develop as further increases in bypass ratio drive shorter inlets. Although challenges remain with regard to icing protection, aerodynamic drag, and inlet off-design performance, it is expected that development of this technology will continue to address these challenges in the Far Term time frame. It is not expected that this technology will be highly effective at the system-level, as the inlet-radiated noise of the ND8 is largely shielded by the fuselage. It is nonetheless included for completeness, as no aspect of the ND8 precludes its use.

With the addition of these technologies, fan noise may be reduced to a level where other noise sources may become

important at the system level. To address core noise, a folding cavity liner can be applied to the center plug of the engine. The perforated face sheet covers the converging section of the core nozzle plug. This feature has been tested previously on a GE CF34 engine [51, 52]. Based on published results, an attenuation of just over 8 dB at 400 Hz, with a rapid roll off at higher and lower frequencies, is applied to core noise at all engine conditions and emission angles.

B. Airframe Technologies

A slat cove filler is applied to address leading edge noise, which is seen as a significant source of noise on approach. Development of a slat cove filler has been ongoing for several years [53], with one enabling technology being the recent advances in shape-memory alloy (SMA) slat cove fillers [54] that can be stowed and deployed automatically as the slats are retracted and extended. The GUO-LE module within ANOPP-Research directly handles the noise of a slat with a cove filler.

In addition to the fairings on the leading edge devices, a further effect is considered in which the gap between the trailing edge of the slat and the leading edge of the main wing is sealed. This could be accomplished using a structure similar to a slat gap filler [55] and would eliminate the high speed flow between the two wing elements that is a significant source of noise for the slat. Of course, sealing this gap runs counter to the high-lift performance benefit of including a slat. However, with continual improvements being made to the aerodynamics of high-lift systems, it is anticipated that this will be a viable configuration in the Far Term time frame. It is noted here that this technology is only required at approach conditions; as with in-service aircraft, it is assumed that no gap would be present during takeoff conditions. The GUO-LE module within ANOPP-Research has the ability to handle a sealed gap configuration, directly computing the noise in this case.

A concept of relevance to trailing edge flap noise is the continuous moldline link (CML) flap. The concept arises from the understanding that one of the primary sources of flap noise is the rollup vortex in the cross flow at the side edge. By effectively blending the flap side edge into the main wing element, the CML flap reduces or eliminates this vortex, achieving significant noise reduction. An acoustic model for this effect is developed by considering both the low- and high-frequency flap side edge noise sources, which scale with flap chord and thickness, respectively. Using data from a small scale wind tunnel test [56], a maximum expected noise reduction for each component is established. A functional roll-off of noise reduction with respect to frequency and directivity angle is then assumed to fill out the model. It is worth noting that the effectiveness of the CML flap within this roadmap study may be tempered by the fact that the baseline aircraft already assumes two low noise concepts as described in Section III, namely the continuous trailing edge flap system that minimizes discontinuities between adjacent flap elements, as well as the porous flap side edge treatment that is considered a Mid Term level technology.

The final prominent noise source to be discussed is the landing gear. Here, vehicle configuration plays a large role in determining the options available for noise reduction. With the ND8's engines above the fuselage, the pod gear concept

[57] presents a feasible alternative to the conventional main gear arrangement. With the gear placed in non-load-bearing pods, which act as large fairings around the complex struts, supports, and hydraulic systems present on the main gear, flow around the gear is smoothed considerably, leading to reduction of noise at the source. In addition, noise absorbing liners placed within the pod cavity help to attenuate any reflected noise from the exposed gear components. Finally, an axle fairing placed around the main gear axle further contains radiated noise within the pod structure. The acoustic impact of this technology is computed using a physics-based method [18] that accounts for the propagation of noise from the main gear structure around the pod and axle fairing. Although the nose gear is not typically a significant noise contributor, it may play a larger role as other noise sources, including the main gear, are attenuated. As such, a partial nose gear fairing is applied as a Far Term technology.

VII. Far Term Aircraft - Results and Discussion

For this roadmap study, the noise reduction technologies shown in Table 5 are evaluated in two ways. The first involves a sequential buildup of technologies, wherein the most effective technology is applied first, followed by the next most effective, and so on. The second method is utilized upon completion of the sequential buildup; once all technologies have been applied, yielding the final Far Term configuration, each technology is removed individually, one at a time, in order to evaluate the effectiveness of that technology on the final configuration. This "one-off" process removes the sequential bias inherent in the first method, and evaluates all technologies on an equal basis.

As mentioned previously, two versions of the ND8 will be carried forward through the roadmap, one including all PAA effects, and one that assumes the acoustic effect of BLI on fan noise is suppressed. Before considering the effects of adding individual technologies, it is useful to examine the ranking of noise sources for each configuration prior to adding Far Term technologies. For this, the reader is directed back to Figs. 11 through 13, which show PNLT curves at each of the three certification points. It is clear that including all PAA effects leads fan noise to dominate the peak PNLT at all three certification points and to be the dominant source at takeoff conditions even to the 10 dB down point relevant to EPNL calculations. This makes it clear that noise reduction technologies applied to other sources will have a minimal impact on the system-level cumulative noise. The possible exception is slat noise on approach, where the engine throttle (and therefore noise) is minimized and slat noise comes within 10 dB of the fan noise.

With the effect of BLI suppressed, fan noise is less dominant at all points, and this presents more opportunities for noise reduction using technologies that target a more diverse set of sources. On approach, slat noise is a dominant source that is within 3 dB of fan noise. Main gear noise is also a significant component of noise, particularly at forward emission angles (as the aircraft approaches the observer). On takeoff, jet noise is within approximately 5 dB of fan noise at the lateral observer. Finally, fan noise still remains dominant at the flyover observer, as this location is most influenced by aft fan noise reflections from the pi-tail.

With these source rankings in mind, now consider the system-level noise impacts of the technologies described

previously. Table 6 shows the results of the sequential buildup and one-off analysis for the ND8 with and without the acoustic BLI penalty. When the acoustic BLI penalty is removed, the noise characteristics and source ranking of the ND8 are altered as described previously. The relative system-level impact of each technology changes in turn. To capture these changes, the table shows the rank change of technologies in terms of system-level effectiveness when the acoustic BLI penalty is removed. Note also that the total impact reported in the last row of Table 6 represents the difference in the cumulative noise levels of the Mid Term and Far Term configurations. The total impact differs from the simple summation of each technology's impact due to the accumulation of rounding errors.

It is clear that the scarf nozzle has the greatest impact on the system noise of the ND8, whether or not BLI is included in the acoustic modeling, due to the dominance of aft fan noise. The over-the-rotor liner also targets fan noise in general, which makes it the second most effective technology for both configurations. It is here that the two configurations begin to diverge in the order of effectiveness for subsequent technologies. With all PAA effects, fan noise is more dominant, and as such, the bifurcation liner has the greatest impact of the remaining technologies. The cove filler follows, along with the PAA liner and pod gear concepts. With BLI suppressed, the cove filler and pod gear are more effective than the bifurcation liner and PAA liner due to the altered source ranking. In fact, the cove filler is nearly twice as effective on an EPNL level on the ND8 with BLI suppressed as it is with all PAA effects included. The center plug liner, sealed slat gap, and nose gear fairing have milder effects, together adding up to 0.5 EPNdB reduction with all PAA effects and 1.0 EPNdB with BLI suppressed. For this aircraft, the CML flap and lip liner have a negligible impact on the noise.

Table 6 System-level impacts of noise reduction technologies on the ND8. Values given are ΔEPNL.

All PAA Effects				BLI Suppressed		
Technology	Buildup	One-Off	Rank Change	Technology	Buildup	One-Off
Scarf Nozzle	-3.4	-3.3	—	Scarf Nozzle	-2.2	-2.5
Over-the-rotor liner	-1.5	-1.7	—	Over-the-rotor liner	-1.3	-1.4
Bifurcation Liner	-0.8	-0.8	↑1	Cove Filler	-1.0	-1.4
Cove Filler	-0.6	-0.7	↑2	Pod Gear	-0.6	-0.7
PAA Liner	-0.6	-0.7	↓2	Bifurcation Liner	-0.6	-0.6
Pod Gear	-0.4	-0.3	↓1	PAA Liner	-0.5	-0.5
Center Plug Liner	-0.2	-0.1	—	Center Plug Liner	-0.3	-0.4
Sealed Gap	-0.2	-0.2	—	Sealed Gap	-0.4	-0.4
Nose Gear Fairing	-0.1	-0.1	—	Nose Gear Fairing	-0.3	-0.3
CML Flap	0.0	0.0	—	CML Flap	-0.1	-0.1
Lip Liner	0.0	0.0	—	Lip Liner	0.0	0.0
Total	-7.9			Total	-7.1	

The effectiveness, or lack thereof, of the CML flap and lip liner, in addition to the predicted effect of the pod gear, warrant some further explanation to put these results in context with the present study. It is important to remember that both the pod gear and CML flap, which are Far Term technologies, replace the partial main gear fairing and porous flap

side edge, which are Mid Term technologies. Furthermore, the flap system is already acoustically modeled assuming the continuous trailing edge architecture that minimizes the discontinuities between flap elements and the main wing. As such, the component-level noise reduction that occurs when transitioning from porous flap side edge to CML flap is much smaller than, for example, if the CML flap were to be applied to an untreated flap with a more traditional design architecture with large discontinuities between elements. This, together with the fact that flap noise is not a dominant source on the ND8, explains the ineffectiveness of this technology, but this is only applicable to this configuration. As main gear noise is a somewhat more dominant source than flap noise, the pod gear registers with a larger effect than the CML flap at the system level. It is still fair to say, however, that the pod gear as applied here to a two-wheel main gear is less effective than the pod gear applied previously [20, 41] to the six-wheel gear featured on larger aircraft, both due to the higher source ranking of gear noise on those larger aircraft, in addition to the higher component-level noise reduction that the pod gear achieves for a six-wheel gear by shielding a much more complex and noisy structure. In a similar way, the lack of any system-level noise reduction by the lip liner is explained simply by the fact that inlet noise is almost entirely shielded by the ND8 fuselage, and is therefore not a noise source that contributes to the overall EPNL. The lip liner can be a useful technology for other configurations where the inlet noise is not shielded.

The results of the one-off analysis are largely consistent with the results of the sequential buildup, signifying that the source ranking of the Mid and Far Term configurations of the ND8 are similar. With all PAA effects included, the complete portfolio of Far Term technologies achieves 7.9 EPNdB of cumulative system noise reduction. Likewise, with the acoustic effect of BLI suppressed, the same portfolio reduces the system noise by 7.1 EPNdB. Considering now the total system noise of the ND8, and how this relates to the NASA Far Term goals, Table 7 shows the final cumulative noise level for the ND8. The Far Term aircraft designates the final configuration with all Far Term noise

Table 7 Cumulative noise margins to certification of the ND8.

	Margin to Stage 4 (Stage 5), EPNdB	
Configuration	Mid Term Aircraft	Far Term Aircraft
NASA Goal	32 - 42	42 - 52
ND8 w/ All PAA Effects	9.4 (2.4)	17.3 (10.3)
ND8 w/ Scattering Only	24.5 (17.5)	31.6 (24.6)
System-Level BLI Penalty	15.1	14.3

reduction technologies applied. With all PAA effects, the portfolio of technologies nearly doubles the ND8 margin to Stage 4, representing a significant improvement overall. With BLI suppressed, the ND8 approaches 32 EPNdB below Stage 4. However, as evidenced by the comparison with NASA goals, this aircraft falls well short of the needed noise performance of future aircraft concepts, particularly the (more realistic) case of the ND8 with all PAA effects included. The acoustic BLI penalty is also presented in Table 7 for both Mid Term and Far Term configurations. It is worth noting here that the acoustic BLI model used in this study has not changed from Mid Term to Far Term, but rather the change

in source ranking between the Mid and Far Term aircraft leads to a difference in the system-level impact of the increased fan noise due to BLI. The reduction in fan noise due to the Far Term technologies results in a lessening of the impact of BLI, from 15.0 to 14.3 EPNdB.

VIII. Conclusion

A comprehensive noise assessment of the NASA D8 concept aircraft has been performed using the NASA research-level Aircraft NOise Prediction Program (ANOPP-Research). This version of ANOPP is well-suited to unconventional aircraft configurations and so provides a strong basis for this noise assessment. The airframe and engine designs of the ND8 were optimized for minimum fuel burn, and this overall design was used without modification for the system noise assessment. Noise reduction technologies and detailed design components appropriate to the 2035 entry-into-service date were assumed. The propulsion-airframe aeroacoustic (PAA) effects of the ND8 were seen to be the defining features in terms of noise, demonstrating that any rigorous and credible noise prediction of this concept must account for these effects. The acoustic effect of boundary layer ingestion, a design feature meant to reduce fuel burn at cruise, was modeled using data from several experiments that featured key physical phenomena - turbulence ingestion and a once-per-revolution variation in fan blade incidence angle. These experiments were chosen because they typically featured turbofans with realistic speeds and pressure ratios. The BLI acoustic model was compared with the results of other studies with turbulence ingestion, some with less realistic fans and others with more limited data available. The results compared well on a qualitative basis and improved confidence in the relative magnitude of the BLI effect predicted by the model. Uncertainty quantification of the acoustic BLI model and how the uncertainty propagates to the system-level uncertainty requires further in-depth study and so is left to future work. The scattering effects (shielding, reflection, and diffraction) were quantified using data from prior experiments, and mapped to reflect the unique geometry of the ND8.

When all Mid Term noise reduction technologies (porous flap side edge, partial main gear fairing, MDOF liner, and soft vane) and PAA effects are included, the ND8 is predicted to have a cumulative margin to Stage 4 certification levels of only 9.4 EPNdB. Boundary layer ingestion is predicted to have a roughly 15 EPNdB noise penalty on cumulative certification noise. The majority of this effect comes from the sideline point, where engines are at full throttle for takeoff. Due to the rotational speed and number of fan blades, the blade passage frequency and harmonics are placed in the 1-4 kHz range where spectral levels have the most influence on tone-corrected perceived noise level (PNLT) and, by extension, EPNL. The strong tonal levels expected due to BLI also result in an additional tone penalty beyond the base increase in source level.

If BLI noise is entirely suppressed, the cumulative margin to Stage 4 is 24.5 EPNdB. The shielding benefit achieved by engine placement is limited by the dominance of unshielded aft-radiated fan noise, particularly at the cutback condition. Reflections from the horizontal tail also contribute to noise in the aft region. The fuselage structure just

upstream of the engines does provide some shielding benefit at sideline, but again, this benefit is limited to forward angles. Further reduction of fan noise would require the addition of more aggressive noise reduction technologies or reconfiguration of the tail layout to accommodate higher bypass ratio engines.

Eleven Far Term noise reduction technologies were later incorporated into the noise assessment to evaluate the ND8's low noise potential in the timeframe of 2035 and beyond. After implementing the acoustic effects of each technology, system-level cumulative noise was reduced by 7.9 EPNdB relative to the Mid Term aircraft when all PAA effects were included in the simulation, whereas the benefit was 7.1 EPNdB for the same set of technologies when the acoustic effect of BLI was suppressed. The technologies of most benefit were those that targeted fan noise, either at the source or by modifying the propagation and scattering. The scarf exhaust nozzle was the most effective, as it reflected fan noise away from ground observers in the aft direction where fan noise was most dominant. Airframe noise reduction technologies tended to be less effective at the system level due to the lower ranking of these sources relative to the fan and jet, although the slat cove filler effectively reduced cumulative levels by 1.0 EPNdB when the acoustic effect of BLI was suppressed.

The unfavorable PAA effects of the ND8, including lack of aft shielding and reflection of aft fan noise, plus the acoustic BLI penalty, lead to high noise levels for the Mid Term aircraft and make it very challenging to meet the Far Term goal after application of the technologies in this study. All of the technologies provide only a 7-8 EPNdB cumulative benefit, compared to the 10 EPNdB difference between the Mid Term and Far Term goals. This means that the ND8 must meet the Mid Term goal to have any chance of meeting the Far Term goal once the Far Term technologies are applied. This study reinforces the conclusion of prior studies on larger aircraft that the best method to reduce overall noise is through a configuration change to gain favorable PAA effects.

Of course, the aircraft configuration should not be the sole focus of noise reduction. Further development, maturation, and expansion of the Far Term technology portfolio is needed to improve the expected noise benefit, in particular for aircraft in this passenger class. Technologies to target the source and propagation of fan noise, especially that which is radiated in the aft direction, such as the scarf nozzle and PAA liner, have the greatest impact at the system level and could provide the most benefit with maturation. However, airframe technologies such as the slat cove filler can also lead to appreciable reductions in system noise, and further development of these technologies is crucial not only to confirm the expected noise benefits, but also to bring about further advancements that can improve their performance. Finally, it must be emphasized that new and innovative concepts must be devised and added to the Far Term technology portfolio in order to improve the possibility of meeting the Far Term goals with any aircraft.

Acknowledgments

The support of the Aircraft Noise Reduction Subproject of the Advanced Air Transport Technology Project is gratefully acknowledged. The authors would like to thank Jason June, John Rawls, and Stuart Pope of the Aircraft

System Noise/PAA Team of the Aeroacoustics Branch at NASA Langley Research Center for their supporting efforts. The engine definitions were provided by the Propulsion Systems Analysis Branch at NASA Glenn Research Center. The airframe and flight path definitions were provided by the Aeronautics Systems Analysis Branch at NASA Langley Research Center. Artist renderings of the aircraft and engines were created and provided by the Advanced Concepts Laboratory, Analytical Mechanics Associates for this study.

References

[1] *Strategic Implementation Plan, 2019 Update*, NASA Aeronautics Research Mission Directorate, 2019.

[2] Greitzer, E. M., Bonnefoy, P. A., De la Rosa Blanco, E., Dorbian, C. S., Drela, M., Hall, D. K., Hansman, R. J., Hileman, J. I., Liebeck, R. H., Lovegren, J., Mody, P., Pertuze, J. A., Sato, S., Spakovszky, Z. S., Tan, C. S., Hollman, J. S., Duda, J. E., Fitzgerald, N., Houghton, J., Kerrebrock, J. L., Kiwada, G. F., Kordonowy, D., Parrish, J. C., Tylko, J., Wen, E. A., and Lord, W. K., "N + 3 Aircraft Concept Designs and Trade Studies, Final Report Volume 1," *NASA/CR—2010-216794/VOL1*, 2010.

[3] Drela, M., "Development of the D8 Transport Configuration," *29th AIAA Applied Aerodynamics Conference*, Honolulu, Hawaii, 2011. doi:10.2514/6.2011-3970.

[4] Yutko, B. M., Jeffrey, C. T., Church, C. S., Courtin, C., Lieu, M., Roberts, T. W., and Titchener, N., "Conceptual Design of a D8 Commercial Aircraft," *17th AIAA Aviation Technology, Integration, and Operations Conference*, Denver, Colorado, 2017. doi:10.2514/6.2017-3590.

[5] Hill, G., and Thomas, R., "Challenges and Opportunities for Noise Reduction Through Advanced Aircraft Propulsion Airframe Integration and Configurations," *8th CEAS Workshop on Aeroacoustics of New Aircraft and Engine Configurations*, Budapest, Hungary, 2004.

[6] Chambers, J. T., Yutko, B. M., Singh, R., and Church, C., "Structural Optimization Study of the D8 Double-Bubble Composite Fuselage," *58th AIAA/ASCE/AHS/ASC Structures, Structural Dynamics, and Materials Conference*, Grapevine, Texas, 2017. doi:10.2514/6.2017-0508.

[7] Marien, T. V., Welstead, J. R., and Jones, S. M., "Vehicle Level System Impact of Boundary Layer Ingestion for the NASA D8 Concept Aircraft," *AIAA SciTech Forum - 56th AIAA Aerospace Sciences Meeting*, Kissimmee, Florida, 2018. doi:10.2514/6.2018-0271.

[8] Pandya, S. A., "Computational Assessment of the Boundary Layer Ingesting Nacelle Design of the D8 Aircraft," *AIAA SciTech Forum - 52nd Aerospace Sciences Meeting*, National Harbor, Maryland, 2014. doi:10.2514/6.2014-0907.

[9] Uranga, A., Drela, M., Greitzer, E. M., Hall, D. K., Titchener, N. A., Lieu, M. K., Siu, N. M., Casses, C., Huang, A. C., Gatlin, G. M., and Hannon, J. A., "Boundary Layer Ingestion Benefit of the D8 Transport Aircraft," *AIAA Journal*, Vol. 55, No. 11, 2017, pp. 3693–3708. doi:10.2514/1.J055755.

[10] Hall, D. K., Huang, A. C., Uranga, A., Greitzer, E. M., Drela, M., and Sato, S., "Boundary Layer Ingestion Propulsion Benefit for Transport Aircraft," *Journal of Propulsion and Power*, Vol. 33, No. 5, 2017, pp. 1118–1129. doi:10.2514/1.B36321.

[11] Uranga, A., Drela, M., Hall, D. K., and Greitzer, E. M., "Analysis of the Aerodynamic Benefit from Boundary Layer Ingestion for Transport Aircraft," *AIAA Journal*, Vol. 56, No. 11, 2018, pp. 4271–4281. doi:10.2514/1.j056781.

[12] De la Rosa Blanco, E., and Hileman, J. I., "Noise Assessment of the Double-Bubble Aircraft Configuration," *49th AIAA Aerospace Sciences Meeting*, Orlando, Florida, 2011. doi:10.2514/6.2011-268.

[13] Preisser, J. S., and Chestnutt, D., "Flight Effects on Fan Noise with Static and Wind-Tunnel Comparisons," *Journal of Aircraft*, Vol. 21, No. 7, 1984, pp. 453–461. doi:10.2514/3.44993.

[14] Alexander, W. N., Devenport, W. J., Wisda, D., Morton, M. A., and Glegg, S. A., "Sound Radiated From a Rotor and Its Relation to Rotating Frame Measurements of Ingested Turbulence," *20th AIAA/CEAS Aeroacoustics Conference*, Atlanta, Georgia, 2014. doi:10.2514/6.2014-2746.

[15] Wisda, D., Alexander, W. N., Devenport, W. J., and Glegg, S. A., "Boundary Layer Ingestion Noise and Turbulence Scale Analysis at High and Low Advance Ratios," *20th AIAA/CEAS Aeroacoustics Conference*, Atlanta, Georgia, 2014. doi:10.2514/6.2014-2608.

[16] Zorumski, W. E., "Aircraft Noise Prediction Program Theoretical Manual," Tech. rep., NASA TM-83199, 1982.

[17] Lopes, L., and Burley, C., "Design of the Next Generation Aircraft Noise Prediction Program: ANOPP2," *17th AIAA/CEAS Aeroacoustics Conference (32nd AIAA Aeroacoustics Conference)*, American Institute of Aeronautics and Astronautics, 2011. doi:10.2514/6.2011-2854.

[18] Guo, Y., Burley, C. L., and Thomas, R. H., "Landing Gear Noise Prediction and Analysis for Tube-And-Wing and Hybrid-Wing-Body Aircraft," *54th AIAA Aerospace Sciences Meeting*, San Diego, California, 2016. doi:10.2514/6.2016-1273.

[19] Guo, Y., Burley, C. L., and Thomas, R. H., "Modeling and Prediction of Krueger Device Noise," *22nd AIAA/CEAS Aeroacoustics Conference*, Lyon, France, 2016. doi:10.2514/6.2016-2957.

[20] Thomas, R. H., Guo, Y., Berton, J., and Fernandez, H., "Aircraft Noise Reduction Technology Roadmap Toward Achieving The NASA 2035 Goal," *23rd AIAA/CEAS Aeroacoustics Conference*, Denver, Colorado, 2017. doi:10.2514/6.2017-3193.

[21] June, J. C., Thomas, R. H., and Guo, Y., "System Noise Prediction Uncertainty Quantification for a Hybrid Wing–Body Transport Concept," *AIAA Journal*, Vol. 58, No. 3, 2020, pp. 1157–1170. doi:10.2514/1.j058226.

[22] Nickol, C. L., and Haller, W. J., "Assessment of the Performance Potential of Advanced Subsonic Transport Concepts for NASA's Environmentally Responsible Aviation Project," *AIAA SciTech Forum - 54th AIAA Aerospace Sciences Meeting*, San Diego, California, 2016. doi:10.2514/6.2016-1030.

[23] *Noise Standards: Aircraft Type and Airworthiness Certification*, Code of Federal Regulations, Title 14, Chapter 1, Part 36, January 2018.

[24] McCullers, L. A., "Aircraft Configuration Optimization including Optimized Flight Profiles," *Proceedings of the Symposium on Recent Experiences in Multidisciplinary Analysis and Optimization, NASA CP-2327*, 1984. URL https://ntrs.nasa.gov/citations/19870002310.

[25] Lytle, J. K., "The Numerical Propulsion System Simulation: An Overview," *NASA/TM-2000-209915*, 2000. URL https://ntrs.nasa.gov/citations/20000063377.

[26] "Design Considerations for Minimizing Hazard Caused by Uncontained Turbine Engine and Auxiliary Power Unit Rotor Failure," *Federal Aviation Administration Advisory Circular 20-128A*, 1997.

[27] Thomas, R. H., Burley, C. L., and Nickol, C. L., "Assessment of the Noise Reduction Potential of Advanced Subsonic Transport Concepts for NASA's Environmentally Responsible Aviation Project," *AIAA SciTech Forum - 54th AIAA Aerospace Sciences Meeting*, San Diego, California, 2016. doi:10.2514/6.2016-0863.

[28] Khorrami, M. R., Humphreys, W. M., Lockard, D. P., and Ravetta, P. A., "Aeroacoustic Evaluation of Flap and Landing Gear Noise Reduction Concepts," *20th AIAA/CEAS Aeroacoustics Conference*, 2014. doi:10.2514/6.2014-2478.

[29] Fares, E., Casalino, D., and Khorrami, M. R., "Evaluation of Airframe Noise Reduction Concepts via Simulations Using a Lattice Boltzmann Approach," *21th AIAA/CEAS Aeroacoustic Conference and Exhibit*, Dallas, Texas, 2015. doi:10.2514/6.2015-2988.

[30] Majumdar, S. J., and Peake, N., "Noise generation by the interaction between ingested turbulence and a rotating fan," *Journal of Fluid Mechanics*, Vol. 359, 1998, pp. 181–216. doi:10.1017/S0022112097008318.

[31] Glegg, S. A. L., Devenport, W., and Alexander, N., "Broadband rotor noise predictions using a time domain approach," *Journal of Sound and Vibration*, Vol. 335, 2015, pp. 115–124. doi:10.1016/j.jsv.2014.09.007.

[32] Envia, E., "Acoustic Power Transmission Loss Through A Ducted Fan," *22nd AIAA/CEAS Aeroacoustics Conference*, Lyon, France, 2016. doi:10.2514/6.2016-3064.

[33] Verdon, J. M., "Linearized Unsteady Aerodynamic Analysis of the Acoustic Response to Wake / Blade-Row Interaction," Tech. rep., NASA/CR-2001-210713, 2001.

[34] Hanson, D. B., "Spectrum of Rotor Noise Caused by Atmospheric Turbulence," *The Journal of the Acoustical Society of America*, Vol. 56, No. 1, 1974, pp. 110–126. doi:10.1121/1.1903241.

[35] Jones, W. L., McArdle, J. G., and Homyak, L., "Evaluation of Two Inflow Control Devices for Flight Simulation of Fan Noise Using a JT15D Engine," *5th Aeroacoustics Conference*, Seattle, Washington, 1979. doi:10.2514/6.1979-654.

[36] "Flight effects of fan noise," *NASA Conference Publication 2242*, edited by D. Chestnutt, 1982. URL https://ntrs.nasa.gov/citations/19830002613.

[37] Clark, L., Thomas, R., Dougherty, R., Farassat, F., and Gerhold, C., "Inlet shape effects on the far-field sound of a model fan," *3rd AIAA/CEAS Aeroacoustics Conference*, Atlanta, Georgia, 1997. doi:10.2514/6.1997-1589.

[38] Koch, L., "An Experimental Study of Fan Inflow Distortion Tone Noise," *15th AIAA/CEAS Aeroacoustics Conference (30th AIAA Aeroacoustics Conference)*, Miami, Florida, 2009. doi:10.2514/6.2009-3290.

[39] Czech, M. J., and Thomas, R. H., "Open Rotor Aeroacoustic Installation Effects for Conventional and Unconventional Airframes," *AIAA Aeroacoustics Conference*, Berlin, Germany, 2013. doi:10.2514/6.2013-2185.

[40] Czech, M. J., Thomas, R. H., and Elkoby, R., "Propulsion Airframe Aeroacoustic Integration Effects for a Hybrid Wing Body Aircraft Configuration," *International Journal of Aeroacoustics*, Vol. 11, No. 3-4, 2012, pp. 335–367. doi:10.1260/1475-472X.11.3-4.335.

[41] Guo, Y., Thomas, R. H., Clark, I. A., and June, J. C., "Far-Term Noise Reduction Roadmap for the Midfuselage Nacelle Subsonic Transport," *Journal of Aircraft*, Vol. 56, No. 5, 2019, pp. 1893–1906. doi:10.2514/1.c035307.

[42] Clark, I. A., Thomas, R. H., and Guo, Y., "Aircraft System Noise Assessment of the NASA D8 Subsonic Transport Concept," *2018 AIAA/CEAS Aeroacoustics Conference*, Atlanta, Georgia, 2018. doi:10.2514/6.2018-3124.

[43] Sutliff, D., Elliott, D., Jones, M., and Hartley, T., "Attenuation of FJ44 Turbofan Engine Noise with a Foam-Metal Liner Installed Over-the-Rotor," *15th AIAA/CEAS Aeroacoustics Conference (30th AIAA Aeroacoustics Conference)*, Miami, Florida, 2009. doi:10.2514/6.2009-3141.

[44] Bozak, R. F., and Dougherty, R. P., "Measurement of Noise Reduction from Acoustic Casing Treatments Installed Over a Subscale High Bypass Ratio Turbofan Rotor," *2018 AIAA/CEAS Aeroacoustics Conference*, Atlanta, Georgia, 2018. doi:10.2514/6.2018-4099.

[45] Howerton, B. M., and Jones, M. G., "Acoustic Liner Drag: Measurements on Novel Facesheet Perforate Geometries," *22nd AIAA/CEAS Aeroacoustics Conference*, Lyon, France, 2016. doi:10.2514/6.2016-2979.

[46] Howerton, B. M., Jones, M. G., and Jasinski, C. M., "Acoustic Liner Drag : Further Measurements on Novel Facesheet Perforate Geometries," *2018 AIAA/CEAS Aeroacoustics Conference*, Atlanta, Georgia, 2018. doi:10.2514/6.2018-3605.

[47] Wong, J. W., Nesbitt, E. H., Jones, M. G., and Nark, D. M., "Flight Test Methodology for NASA Advanced Inlet Liner on 737MAX-7 Test Bed (Quiet Technology Demonstrator 3)," *25th AIAA/CEAS Aeroacoustics Conference*, Delft, The Netherlands, 2019. doi:10.2514/6.2019-2763.

[48] Nark, D. M., and Jones, M. G., "Design of an Advanced Inlet Liner for the Quiet Technology Demonstrator 3," *25th AIAA/CEAS Aeroacoustics Conference*, Delft, The Netherlands, 2019. doi:10.2514/6.2019-2764.

[49] Thomas, R. H., Czech, M. J., and Doty, M. J., "High Bypass Ratio Jet Noise Reduction and Installation Effects Including Shielding Effectiveness," *51st AIAA Aerospace Sciences Meeting*, Grapevine, Texas, 2013. doi:10.2514/6.2013-541.

[50] Yu, J., Hwa-wan, K., Chien, E., Ruiz, M., Nesbitt, E., Uellenberg, S., Premo, J., and Czech, M., "Quiet Technology Demonstrator 2 Intake Liner Design and Validation," *12th AIAA/CEAS Aeroacoustics Conference*, Cambridge, Massachusetts, 2006. doi:doi:10.2514/6.2006-2458.

[51] Yu, J., and Chien, E., "Folding Cavity Acoustic Liner for Combustion Noise Reduction," *12th AIAA/CEAS Aeroacoustics Conference*, Cambridge, Massachusetts, 2006. doi:10.2514/6.2006-2681.

[52] Martinez, M. M., "Determination of Combustor Noise from a Modern Regional Aircraft Turbofan Engine," *12th AIAA/CEAS Aeroacoustics Conference*, Cambridge, Massachusetts, 2006. doi:10.2514/6.2006-2676.

[53] Streett, C. L., Casper, J. H., Lockard, D. P., Khorrami, M. R., Stoker, R. W., Elkoby, R., Wenneman, W. F., and Underbrink, J. R., "Aerodynamic Noise Reduction for High-Lift Devices on a Swept Wing Model," *44th AIAA Aerospace Sciences Meeting and Exhibit*, Reno, Nevada, 2006. doi:10.2514/6.2006-212.

[54] Turner, T. L., Kidd, R. T., Hartl, D. J., and Scholten, W. D., "Development of a SMA-Based, Slat-Cove Filler for Reduction of Aeroacoustic Noise Associated with Transport-Class Aircraft Wings," *ASME 2013 Conference on Smart Materials, Adaptive Structures and Intelligent Systems*, Snowbird, Utah, 2013. doi:10.1115/SMASIS2013-3100.

[55] Turner, T., and Long, D., "Development of a SMA-Based, Slat-Gap Filler for Airframe Noise Reduction," *23rd AIAA/AHS Adaptive Structures Conference*, Kissimmee, Florida, 2015. doi:10.2514/6.2015-0730.

[56] Hutcheson, F., Brooks, T., and Humphreys, W., "Noise Radiation from a Continuous Mold-Line Link Flap Configuration," *International Journal of Aeroacoustics*, Vol. 10, No. 5&6, 2011, pp. 565–588. doi:10.1260/1475-472X.10.5-6.565.

[57] Thomas, R. H., Nickol, C., Burley, C. L., and Guo, Y., "Potential for Landing Gear Noise Reduction on Advanced Aircraft Configurations," *22nd AIAA/CEAS Aeroacoustics Conference*, 2016, pp. 1–12. doi:10.2514/6.2016-3039.